UNIVERSITÀ DEGLI STUDI DI PADOVA

DIPARTIMENTO DI INGEGNERIA INDUSTRIALE

CORSO DI LAUREA MAGISTRALE IN INGEGNERIA CHIMICA E DEI PROCESSI INDUSTRIALI

Tesi di Laurea Magistrale in Ingegneria Chimica e dei Processi Industriali

INKJET PRINTING OF NIROGACESTAT LOADED MESOPOROUS SILICA NANOPARTICLES

Relatore: Prof. Paolo Canu

Correlatore: Prof. Jessica Rosenholm

Laureando: MARCO LAGO

ANNO ACCADEMICO 2018-2019

COPYRIGHT

Turku, August 2018

Supervisor	Author
Jessica Rosenholm	Marco Lago

Alla mia vecchia roccia

Abstract

The focus of this work was to test the printability of drug loaded mesoporous silica nanoparticles (MSNs) as a nano-ink formulation. MSNs were surface functionalized with polyethylenimine (PEI) to inhibit particles aggregation and to enhance the particles uptake in the cancer cells. A pharmaceutical ink made up of MSNs dispersed in a 20:20:60 vol% of water, propylene glycol (PG) and isopropanol (IPA) was developed after having tested several different formulations to ensure fluid stability and accuracy after printing and to avoid that premature drug leaching takes place. The ink base consisting of only solvents and the nano-ink suspensions with both unloaded as well as drug-loaded MSNs (1 mg/mL) were printed. The suspensions were printed on two substrates made by two materials with different absorption properties, varying the printing resolution from 100 to 500 droplets per inch (DPI).

Physicochemical properties of mesoporous silica nanoparticles affect drug loading capacity, colloidal stability and interactions with loaded drugs, leading to different biopharmaceutical profiles with a significant impact on patient safety and therapeutic efficacy. For this reason, several techniques were used to evaluate them.

Printed samples were subjected to confocal scanning laser microscopy (CSLM). This led to the conclusion that nanoparticles, for resolution lower than 300 DPI, appear not homogenously spread on the droplet, giving rise to a deposit along the perimeter of it.

The aim of the project was also to define if CLSM could be used to evaluate the concentration of MSNs and to see if there's an increase of fluorescence signal at higher printing resolution.

This study confirms that drop on demand ink jet printing ensures high precision, since no fluorescence traces were disposed between the printed wheel. However, optimization of the printer is needed to ensure reproducibility, which is essential to offer individual treatments solutions.

Riassunto

L’obiettivo di questo lavoro è stato quello di testare la capacità di stampa di nanoparticelle di silice mesoporosa (MSNs), formulate sotto forma di inchiostro. Queste particelle sono state funzionalizzate superficialmente con un rivestimento in polietilenimmina in modo tale da inibirne l’aggregazione e facilitarne l’assorbimento da parte delle cellule tumorali.
L’inchiostro è stato ottenuto disperdendo le nanoparticelle in una soluzione costituita da acqua, glicole propilenico e isopropanolo rispettivamente in percentuali volumetriche pari a 20:20:60. Questa formulazione è stata sviluppata dopo aver testato diverse altre opzioni in modo tale da assicurare la stabilità del fluido durante lo stampaggio e l’accurata disposizione delle particelle sul substrato scelto; inoltre, la scelta è ricaduta su tale formulazione per evitare la lisciviazione del farmaco dalle particelle dovuta alla solubilità nel solvente dello stesso. Sia la formulazione scelta, sia le particelle cariche o meno disperse nella formulazione stessa, sono state stampate.
Queste sospensioni sono state stampate su due substrati costituiti da due materiali diversi aventi diverse proprietà di assorbimento, variando la risoluzione di stampa da 100 a 500 DPI.
Le proprietà fisico-chimiche delle nanoparticelle di silice mesoporosa influenzano la capacità di caricamento del farmaco, la stabilità colloidale e l’interazione col farmaco stesso, dando luogo a diversi profili biofarmaceutici con un impatto significativo sulla sicurezza del paziente e sull’efficacia della terapia. Per questo motivo, diverse tecniche sono state utilizzate per caratterizzare le particelle.
I campioni stampati sono stati analizzati con il microscopio confocale a scansione laser (CLSM). Ciò ha indotto a concludere che le nanoparticelle, per risoluzioni inferiori a 300 DPI, non sono ben distribuite nella goccia, dando luogo ad un deposito lungo il perimetro della stessa. L’obiettivo del progetto è stato anche valutare se il CLSM poteva essere utilizzato per determinare la concentrazione di MSNs e vedere se una maggior risoluzione di stampa comportasse l’aumento del segnale di fluorescenza. Questo studio conferma che lo stampaggio a getto d’inchiostro *on demand* assicura un’elevata precisione, visto che non ci sono tracce fluorescenti fuoriuscenti dallo schema di stampaggio.
Tuttavia, è necessaria un’ottimizzazione del processo di stampaggio in modo da poter garantire una maggiore riproducibilità, che risulta essere fondamentale per offrire trattamenti personalizzati.

Table of Contents

Abstract **5**

Riassunto **6**

Introduction **9**

1. REVIEW OF THE LITERATURE **11**
1.1 Nanotechnology and synthesis approaches **11**
1.2 Sol gel process **11**
1.3 Porous Network Formation **13**
1.4 Piezoelectric Inkjet Printing **14**

2. MATERIALS AND METHODS **17**
2.1 Mesoporous Silica Nanoparticles Synthesis **17**
2.1.1 Choice of the co-solvent 17
2.1.2 Choice of the silica source 18
2.1.3 Choice of the catalyst 19
2.1.4 Choice of the water and ratio H_2O/Si 21
2.1.5 Choice of the directing agent 23
2.1.6 FITC and APTES 23
2.1.7 Choice of the temperature 26
2.1.8 Choice of the stirring velocity 26
2.1.9 Synthesis Procedure 26
2.2 Mesoporous Silica Nanoparticles Extraction **27**
2.2.1 Choice of the template removal technique 27
2.2.2 Extraction Procedure 27
2.3 Mesoporous Silica Nanoparticles Characterization **28**
2.3.1 Dynamic Light Scattering 29
2.3.2 Zeta Potential 30
2.3.3 TEM 32
2.3.4 Concentration 33
2.3.5 Thermogravimetric Analysis 33
2.3.6 Nitrogen Adsorption 33
2.4. MSNs Surface Functionalization **34**
2.4.1 Methods 35
2.4.2 PEI grafting 35
2.4.3 Reactions and steps involved 36
2.5 Ink Development **37**
2.5.1 Ink Formulation 37
2.5.2 Printing 38
2.6 Ink Characterization **39**
2.6.1 Viscosity 39
2.6.2 Surface Tension and Contact Angle 39
2.6.3 Density 39
2.6.4 Confocal Laser Scanning Microscopy 39
2.6.5 UV – Vis Spectroscopy Analysis 40
2.7 Drug **40**
2.6.1 Drug Formulation 40
2.6.2 Drug Loading 41
2.6.3 Drug Leaching in ink 41

3. RESULTS 43
3.1 MSNs Characterization 43
3.1.1 Size distribution and Zeta Potential of MSNs 43
3.1.2 Effectiveness of surface functionalization 45
3.1.3 Transmission Electron Microscopy of MSNs and concentration 46
3.2 Drug Analysis 48
3.2.1 Uv-Vis Analysis 48
3.2.2 Nirogacestat calibration curve 49
3.3 Ink Characterization 50
3.3.1 Ink Constituents 50
3.3.2 Ink Characterization results 51
3.4 Drug Leaching 53
3.5 Printing Process and droplet analysis 55
3.5.1 Optimization of Printing Settings 55
3.5.2 Dose Quantification 56
3.5.3 Substrate Interactions 57
3.6 Printed Samples Characterization 58
3.6.1 Fluorescence Confocal Microscope 58
4. DISCUSSION 61
4.1 MSNs Characterization 61
4.2 Ink base Properties 63
4.3 Drug Leaching 64
4.4 Printed Samples 65
5. CONCLUSION 67
6. SYMBOLS AND ABBREVIATIONS 69
7. REFERENCES 71
8. APPENDIX 77
Acknowledgement 81

Introduction

The application of nanotechnology in the medical field and the development of theranostic, combining new target nanopharmaceutical formulations and nanodiagnostic technologies, can open new possible pathways for patient's diagnosis and therapy.

Nanopharmaceuticals are able to overcome the limitations associated with the traditional drug therapies, enhancing the efficacy of Active Pharmaceutical Ingredients (API), that before were unsuitable because solubility and precise targeting issues. Protection of the drug against the reticuloendothelial system (RES) or other forms of degradation, high drug loaded capacity and a longer circulation time are the main advantages that the drug encapsulation, in surface functionalized nanomaterials, guarantees.

The awareness of specific individual dose regimens matured by the population and the interest in innovative and fast medical solutions meet with printing, that enables a flexible production. In this context, two dimensional piezoelectric inkjet printing is an additive manufacturing technology that is proposed to facilitate the dose adjustment of nirogacestat loaded mesoporous silica nanoparticles.

1. REVIEW OF THE LITERATURE

1.1 Nanotechnology and synthesis approaches

Formulation approaches utilizing MSNs allow targeting of the medication to the site of action and controllable release of the drug.[1]

Utilization of nanomaterials involves a broad spectrum of clinical applications, ranging from the field of drug delivery to the development of implants, and ensures to overcome the limitations associated with the traditional drug therapies.

There are two general approaches to the synthesis of nanomaterials, the top-down approach and the bottom-up approach. The top-down methods, i.e. lithography and photolithography, use macroscopic initial structures that can be externally controlled to process nanostructures. By nature, these methods are not cheap and slow, resulting not suitable for large scale production. Bottom-up approaches include the miniaturization of materials up to atomic level, with further self-assembly process leading to the formation of nanostructures.

1.2 Sol gel process

The sol-gel method is used to prepare nanosized mesoporous silica nanoparticles. The process begins from nucleation and continues with growth and aggregation.[1] During nucleation, nanoparticles are firstly formed by three equilibrium reactions, hydrolysis (the opposite is an esterification), alcohol condensation (alcoholysis) and water condensation (hydrolysis), and then they aggregate in cyclic structures.

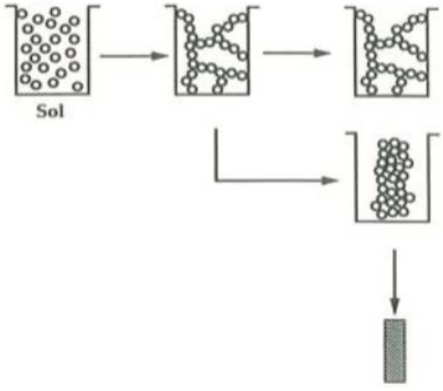

Fig. 1.1. Sol-gel process.[1]

After the Ostwald ripening process and the consequential growth of the crystals, nanoparticles aggregate in order to form porous networks. So, the sol-gel materials are prepared by initially developing a colloidal suspension (called sol), that then proceeds to form a branched network (called gel).[2]

The choice of the substances involved in the sol-gel synthesis of silica mesoporous nanoparticles is done in order to maximize the number of Si-O-Si bonds formed, further promoting a ring formation that leads every single monomer to form a three-dimensional structure.
The obtained particles, due to a thermodynamically driven spontaneous process per which the small particles are more energetic compared to bigger ones just formed after the 'polymerization' process, redeposit on larger particles causing the particles growth. An overview of the scheme of the process can be seen in Figure 1.1.

Hydrolysis

$$\equiv Si-OR + H_2O \rightleftharpoons \equiv Si-OH + ROH$$

Alcohol condensation

$$\equiv Si-OR + HO-Si\equiv \rightleftharpoons \equiv Si-O-Si\equiv + ROH$$

Water condensation

$$\equiv Si-OH + HO-Si \rightleftharpoons \equiv Si-O-Si\equiv + H_2O$$

Fig. 1.2. Reactions involved in mesoporous silica nucleation.[1]

To make silica nanoparticles work effectively as a drug delivery system, it's necessary to synthesize size controllable and monodisperse silica nanoparticles. However, many studies[3,4] have demonstrated how, modifying the process parameters, such as temperature, pH, H_2O/Si molar ratio, stirring velocity, relative substances amount, nature and concentration of the catalysts, type of the silica precursor, could widely vary the final features of the sol gel products.
Nevertheless, even if this could be an advantage since it is theoretically possible to obtain a nanosystem with specific characteristics, during the years several attempts to generate monodisperse suspensions of silica nanoparticles have shown how very often, being exposed to many affecting factors, the size is not precisely reproducible.[57] In fact, each single perturbation of the previously cited parameters could affect irredeemably the size of the particles and not make them useful anymore for the pharmaceutical purpose for which they are made, even causing toxicity issues.
Several investigations were led to understand how to control the complex interplay between all these process parameters.

1.3 Porous Network Formation

Mesoporous silica nanoparticles have been synthesized through a modified Stöber process, using tetraethyl orthosilicate (TEOS) as precursor and cetyltrimethylammonium bromide (CTAB) as surfactant, in solution with water, ethanol (CH_3CH_2OH) and sodium hydroxide (NaOH) as catalyst.[12] CTAB is stirred in a mixture of water and ethanol under pre-defined conditions and TEOS is then added under stirring. Concentration and composition of silica source (in this case TEOS), template agent (CTAB) and environment conditions affect the result, in terms of shape and size of the particles. CTAB is the structure directing agent. It forms micelles in the solution and these will further form a two-dimensional hexagonal structure. The micelles structure is basically formed by hydrophobic and hydrophilic ends, with hydrophobic heads that go inwards, while hydrophilic ends go outwards. Then the TEOS, which is the silica precursor, will hydrolyze and condensate (Figure 1.3) between these micelles and will fill the gap with silicon dioxide forming a silica structure all around.

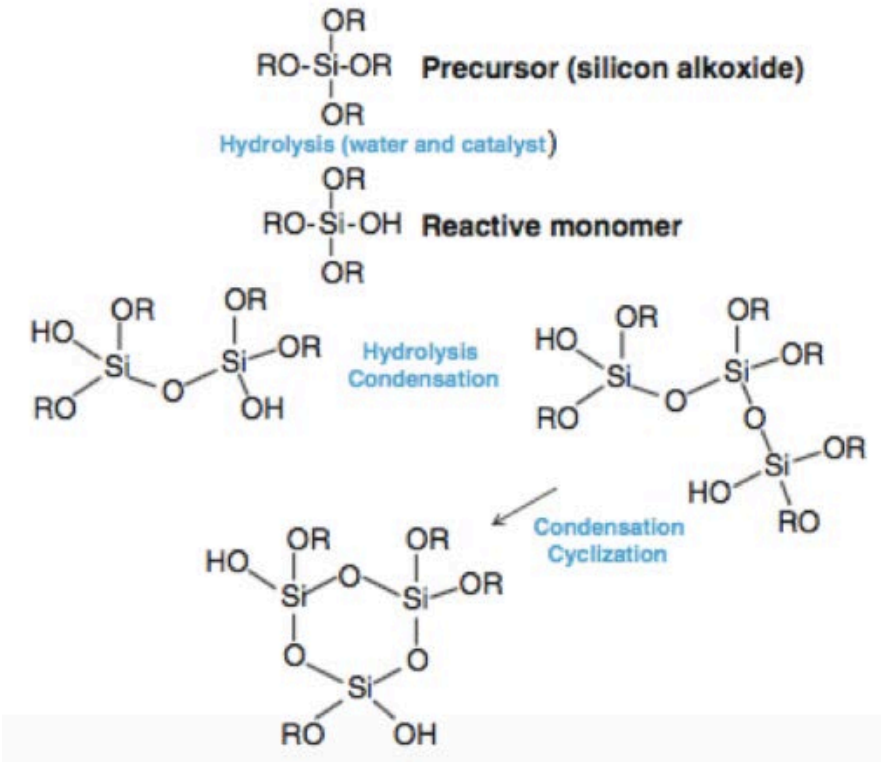

Fig. 1.3. Formation of cyclic structures during sol – gel process.[10]

In order to be able to lead a live cells imaging, making the particles visible under confocal microscopy, and a proper theranostic evaluation, the synthesized nanoparticles were labelled through a FITC co-condensation process. This project included five synthesis, one regarding bare mesoporous silica nanoparticles, two 1% APTES-FITC MSNs of different volumes, and one batch for both 5% and 10% APTES-FITC MSNs.

Bare nanoparticles have been synthesized, even if they are not detectable under confocal microscope, just to check if the procedure was effectively working or not. For further proceedings in the project, the credibility of the nanoparticles was assessed using a wide variety of characterization techniques, including transmission electron microscopy, thermogravimetric analysis, particle sizing and Uv-Vis analysis.

1.4 Piezoelectric Inkjet Printing

Printing helps to accurately dose the particles. The debut of it in pharmacy was just a matter of time and during the last few years the pharmaceutical industry has been increasingly showing the interest for printing technologies.

Piezoelectric Inkjet Printing (PIJ) is used to deposit ink formulations on substrates. In piezoelectric print head, microscopic piezoelectric elements are built behind the print nozzles. When an electrical charge is applied to them, these elements expand, forcing precise amount of ink onto the substrate. When the transducer return to its normal shape, the nozzles are refilled again with the ink from the reservoir (Figure 1.4).

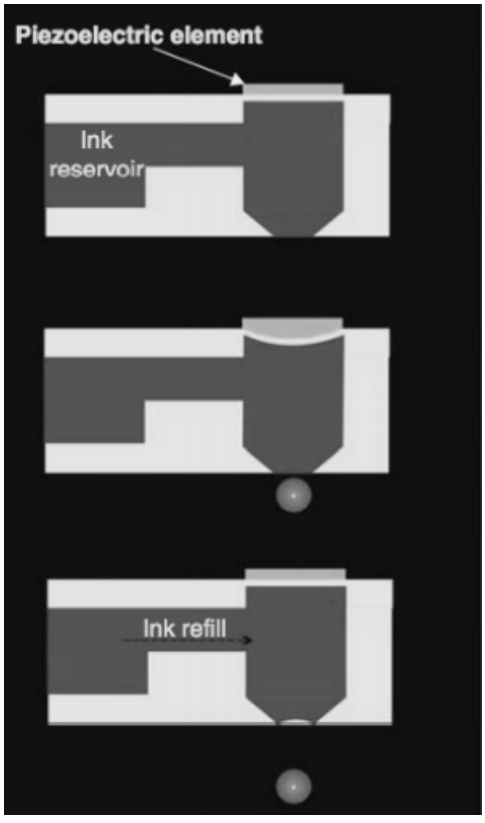

Fig. 1.4. Schematic process of Piezoelectric Inkjet Printing.[23]

The process of formation of the droplets involves an initial generation of pressure that causes the fluid ejection, followed by a round head formation of the filament. Subsequently, a necking due to the different travelling velocity between the filament and the droplet head is produced, until the rapture of the fluid tail, still attached to the nozzle tip.

After that, dependent on physical fluid parameters, such as viscosity, density and surface tension, and on printer head characteristics, like the characteristic dimension of the nozzles and the average travel velocity generated by the pulse, several droplet formation mechanisms may occur.

Z value 'mimic the process' and it had been used to get an indication of printability. Z value is the inverse of the Onhesorge number (Oh), which is the ratio between the square root of the Weber (We) number and the Reynolds number (Re), relating the viscous forces to inertial and surface tension forces. Indicating ρ as density, η as viscosity, γ as surface tension, v as the average travel velocity of the droplet ejected and α as the nozzle radius:

$$Re = \frac{\rho v \alpha}{\eta} \qquad We = \frac{v^2 \rho \alpha}{\gamma} \qquad Z = \frac{Re}{\sqrt{We}} = \frac{\sqrt{\rho \alpha \gamma}}{\eta}$$

For Z values lower than 4 the fluid ejected results in long-lived filament, characterized by a long time to single droplet recombination. If the fluid exhibits a value of Z higher than 14 it's also inappropriate for ink-jet printing because the satellite droplet, formed after the piezoelectrically induced pressure, it's not able to merge with the primary droplet, deteriorating the printing accuracy. However, for values below 6 the initial elongation and breakage of the fluid is rapidly healed to minimize the surface area, while for values between 7 and 13 two droplets are generated and then more rapidly than the previous case merged.

So, between the two boundary values of Z (4 and 14), even if the velocity of filament elongation is different as well as the rapture time, the printing shows ability to deposit the pharmaceutical ink in form of droplets.[42]

However, a formulation characterized by a Z value inside the desired range not necessary ensures a fine jettability. This is due to the fact that different ink compositions can lead to the same Z value. To have a better understanding of the correlation between the formation and the shape of the droplets and the fluid properties, v should be taken into account. Based on previous studies[43], a good positioning accuracy for the pattern could be obtained for Z values between 5 and 9.

2. MATERIALS AND METHODS

2.1 Mesoporous Silica Nanoparticles Synthesis

Hexadecyltrimethylammonium bromide (CTAB) (≥ 99%), tetraethyl orthosilicate (TEOS) (≥ 99%), fluorescein isothiocyanate (FITC) and aminopropyl triethoxysilane (APTES) (≥ 99%) were purchased from Sigma Aldrich Corporation (USA). Sodium hydroxide (NaOH) was purchased from Merck KGaA (USA).

2.1.1 Choice of the co-solvent

The effect of the alcohol type on the synthesis step, that many researchers have reported it is the rate determining step of the entire process[7], is fundamental. Through a GC analysis it was noticed that TEOS, generally reacting with alcohols, changes to other compounds, the silicon alkoxides, also called alkoxisilanes, $Si(OEt)_{4-n}(OMe)_n$[9]. Testing the MSNs synthesis using C_1-C_5 alcohols, was noticed that the particles diameters increased a lot over C_2. The slowest exchange rate, that occurs with the increase of the steric hindrance for C_3, C_4, C_5 alcohols, gives rise to bigger seeds compared to those ones obtainable in methanol (C_1) or ethanol (C_2) ambient.

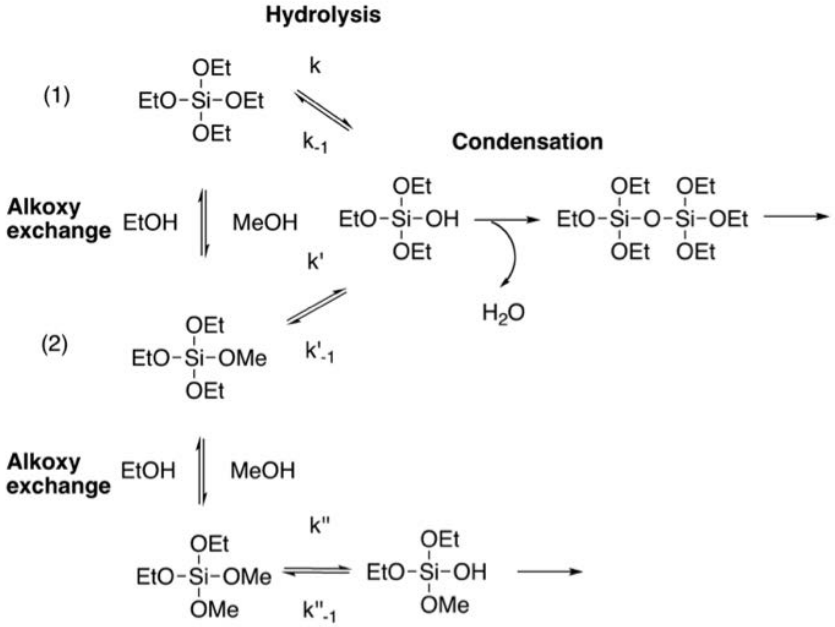

Fig. 2.1. Reactions involved between silica precursor and co-solvent.[6]

Moreover, even for these last two chemicals, the same principle is respected and many smaller seeds, that then will turn to smaller silica porous nanoparticles, were generated in methanol than ethanol

environment. This is due to a completely different path and rate of condensation and hydrolysis reactions that take place during the synthesis.

As illustrated by Joohyun Lim et al. (2012) in Figure 2.1, when it is used a co-solvent mixture, in that case a solution made by methanol and ethanol, the methoxy exchange reaction can compete to hydrolysis and for that some portion of TEOS is changed to $Si(OEt)_3$ (OMe). Since the hydrolysis rate constant of TMOS, Si $(OCH_3)_4$, is known to be more than four times faster than TEOS[6], this methoxy-exchanged silicon compound, that with only one substitution isn't still TMOS but it is something in between TEOS and TMOS, can hydrolyze faster than TEOS (k' > k). For that reason, the more methoxy groups are exchanged on the Si site, faster the hydrolysis occurs, and faster super-saturation point is reached starting to form smaller seeds. Monitoring this with the gas chromatography, was possible to state that the methoxy exchange rate of TEOS is decreased when the amount of ethanol is increased, giving rise to bigger particles.

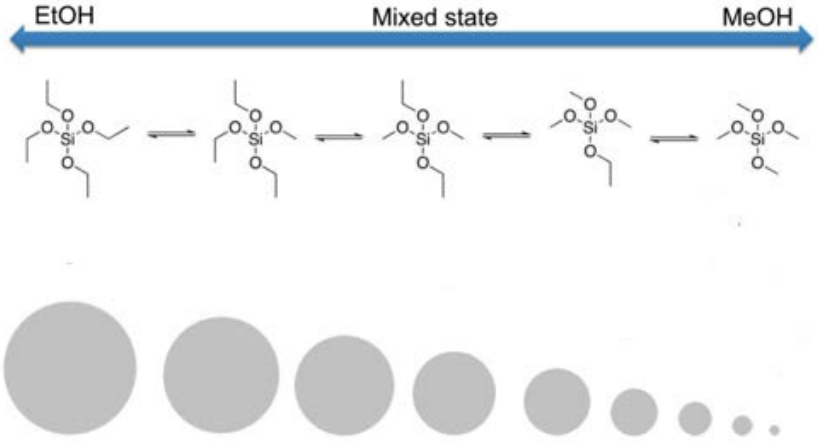

Fig. 2.2. Size differentiation based on the co-solvent mixture.[6]

We have used only ethanol for safety reasons. The more toxicity of methanol compared to ethanol ones means that to ensure safe working conditions, with methanol a proper ventilation is required and it can be handled only by people that have been properly trained.[8]

2.1.2 Choice of the silica source

In general, the silica source could be either an inorganic metal salt or a metal alkoxide. Since there is a huge availability of papers in literature concerning the use of metal organic compounds as precursors and since they react easily with water, we decided to handle them. In particular, in this class we opted for the silicon alkoxides as they are more reactive than the transition metal alkoxides.[10] The most widely used in literature are tetraethylorthosilicate TEOS, $Si(OC_2H_5)_4$, and tetramethylorthosilicate TMOS, $Si(OCH_3)_4$.

We have chosen TEOS because TMOS is less safe to handle and it hydrolyses more quickly, producing too much small nanoparticles that cannot be loaded with the proper drug cargo (Figure 2.3).

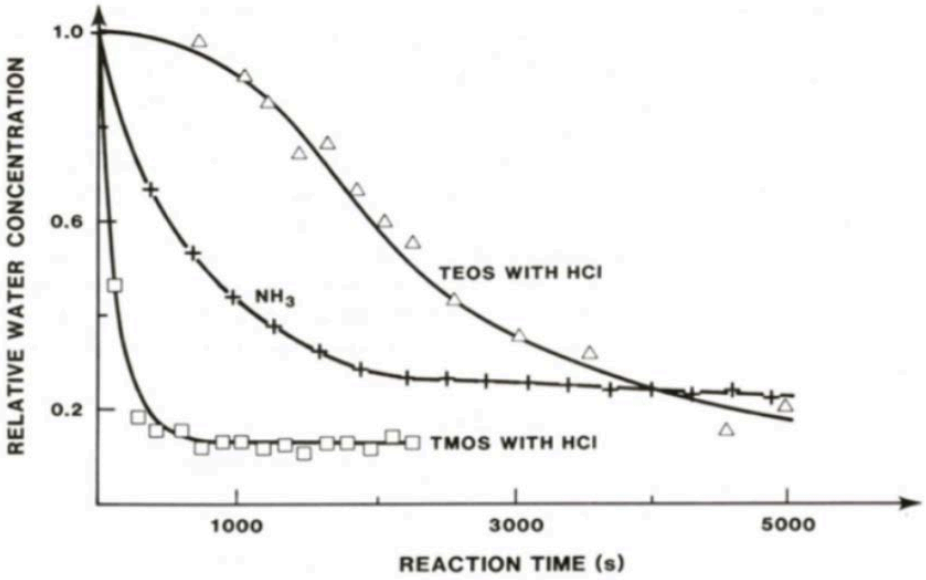

Fig. 2.3. TEOS vs TMOS hydrolysis rate.[60]

As mentioned earlier in the 1.3 section, the silica source is diluted in a solution made by water and ethanol. In this study, we have chosen TEOS and the synthesis solution is majorly composed of ethanol and water, since, as explained in section 2.1.1, if the synthesis is not performed using the alcohol corresponding to the alkoxy group of the silica source, many exchange reactions between the precursor and the co-solvent could occur, modifying the kinetic of the entire process.
Comparing different silica sources, several tests have shown that maintaining the same conditions, the increase of tetraalkoxysilanes molecular weight (MW_{TEOS}=208.33 g/mol, MW_{TMOS}=152.22 g/mol) slows down the condensation, producing particles of larger but uniform size.[4] In order to increase the condensation rate, higher alcohols as co-solvent could be used but this is going to negatively affect (increase) the size of the particles.
For the necessity to find a trade-off, we decided to use TEOS as precursor to guarantee a narrow size distribution and ethanol was preferred as co-solvent for safety reasons and also as it is an intermediate alcohol to achieve the desired size of the nanoparticles required for this study.

2.1.3 Choice of the catalyst

Hydrolysis and condensation reactions, and of the final sol structure, mostly depends on the nature of the catalyst, concentration of the catalyst, and pH. There are few reports that mention the synthesis of mesoporous silica nanoparticles (MSNs) was carried out under acidic conditions, because in this ambient the control of nucleation reaction and particles growth is difficult.[1]
The pathways in these two, basic and acidic, conditions are radically different. In case of acid catalyst

there will be the protonation of the oxygen atom of Si-OR group by the protons of the catalyst available in solution, causing an increase of the positive charge of the silicon, that becomes more electrophilic.
At this point, it is more reactive to the attack of water (hydrolysis) or silanols (condensation):

Hydrolysis $\equiv Si - OR + H^+ \leftrightarrow \equiv Si - O^+ - RH \rightarrow \equiv Si - O^+ - RH + HOH \rightarrow \equiv Si - OH + ROH$

Condensation $\equiv Si - OH + H^+ \leftrightarrow \equiv Si - O^+H - H \rightarrow \equiv Si - O^+R - H + Si - OH \rightarrow \equiv Si - O - Si \equiv$

In basic conditions, the reaction starts because of the intrinsic nucleophilicity of the catalyst, which directly attacks the silicon atom of the precursor. Here the silicon of the metal alkoxide has positive charge and so the deprotonated hydroxiles (HO^-), from the water reaction with the catalyst, attacks it (a). The same happens for the deprotonated silanol (SiO^-), formed before, that reacts with another silanol (b). The reaction below can happen also with an alkyl group instead of H:

$$\equiv Si - OR + HO^- \leftrightarrow (\equiv SiOR - OH)^- \leftrightarrow \equiv Si - OH + RO^- \quad (a)$$

$$\equiv Si - OH + \equiv SiO^- \leftrightarrow (\equiv SiOH - SiO^-)^- \leftrightarrow \equiv Si - O - Si \equiv + HO^- \quad (b)$$

Considering the graph below (Figure 2.4 (a)), that correlates the sol stability gel time with the pH, three pH domains can be identified. The value of pH 2 approximately corresponds to the point of zero charge (PZC). For pH > PZC, the surface is negatively charged, instead for pH < PZC it's positively charged. The pH of the solution will change with the degree of condensation and depends on the specific catalyst. Above pH = 7 particles growth occurs, no aggregation or gel formation are observed because the solubility (Figure 2.4 (b)) and dissolution rates of the particles are maximized due to their ionization.

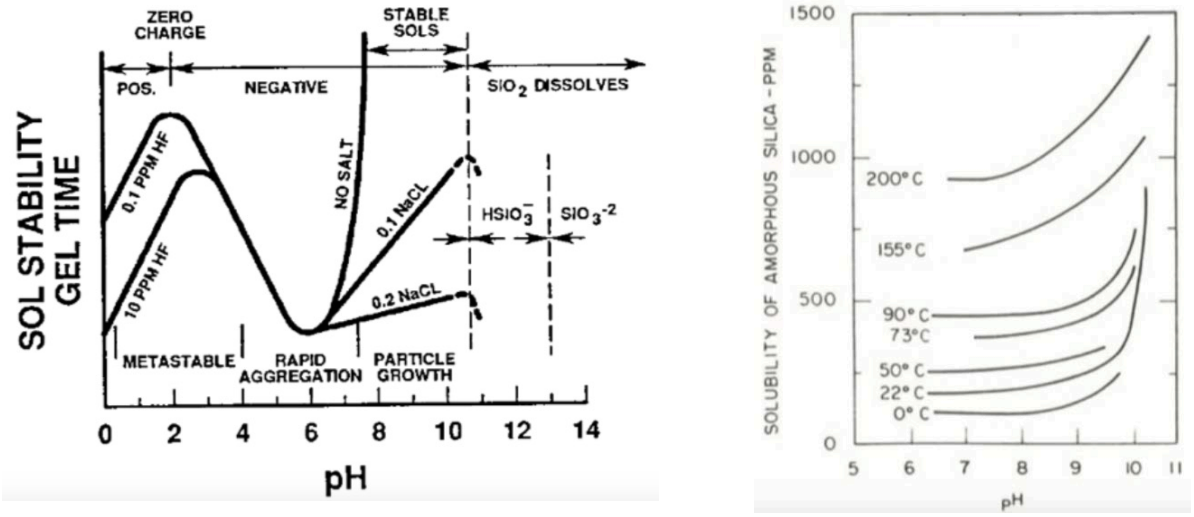

(a) (b)

Fig. 2.4. (a) Sol stability gel time vs pH.[61] (b) Solubility of amorphous silica vs pH.[1]

At these values, in fact, negatively charged particles repeal each other and prefer growing.[2] For the

gelation time is possible to see a maximum stability at PZC, instead for other pH values the time between the addition of the catalyst and the formation of the gel is lower. For low values (pH < 2) the solubility is low (Figure 2.4 (b)) and gel times are long.[1]

Experiments by Plinio Innocenzi (2016) have shown how using basic conditions can allow to obtain a more porous network final material, with more free spaces between the particles, compared to the denser matrix that can be obtained using acidic conditions.[10]

High pH values, independently from the TEOS amount, are essential to obtain a highly ordered mesostructured that we need to get for a homogeneous drug delivery.[11] So, for these reasons, we have chosen to perform the synthesis under basic pH condition, i.e. between 7 and 10, using NaOH as a catalyst. Performing a kinetic study of the process, this basic catalyzed nanosystem leads to a rate of condensation faster than that one of hydrolysis leading to a very branched final structure.[3,10]

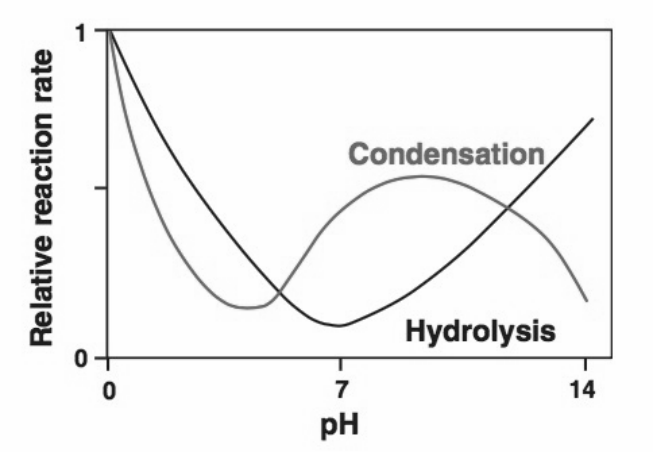

Fig. 2.5. Comparison between condensation and hydrolysis rate varying pH.[10]

2.1.4 Choice of the water and ratio H_2O/Si

De ionized water is used in order to avoid any ions interaction with the reaction solution. The amount of water that is available to start the hydrolysis will have an impact on the morphology of the particles. The stoichiometric water/metal alkoxide ratio (r) is 4; it means that four molecules of water are needed to completely hydrolyze a tetravalent silica precursor, as TEOS.[10] Apparently, an increase of the amount of water could enhance hydrolysis rate and this happens for little positive variation of water; however, as we can see from Figure 2.6, this is not true anymore when r > 5. In this case, in fact, the less concentration of TEOS, due to the dilution with water, is more effective and the gelation time irredeemably increases.[10]

To completely understand the influence that water has on the simultaneous reactions that take place, since it's involved in all the three reactions of Figure 1.2, a detailed kinetic analysis should be done; as C. J. Brinker (1988) discovered, if r < 4 the alcohol condensation is favored, while if r > 4 the water condensation is favored because of the presence of Si-OH.

However, if the excess of water is huge, the depolymerization of linkages Si-O-Si is favored because water becomes the reagent of the hydrolysis.[15]

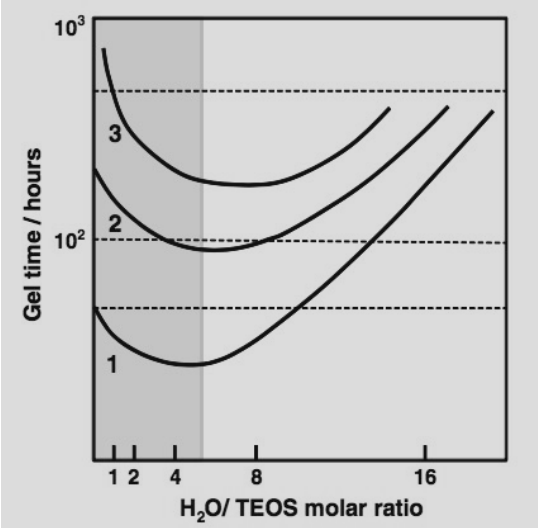

Fig. 2.6. Gel time vs r.[10]

Another important aspect to remind during the choice of the right amount of the substances is the TEOS-ethanol-water ternary diagram. In fact, an enormous adding of water could apparently lead the system to an immiscible phase, but the polycondensation reactions (ref. to Figure 1.2) produce also alcohol as by product, that is enough to keep the solution homogeneus.[10]

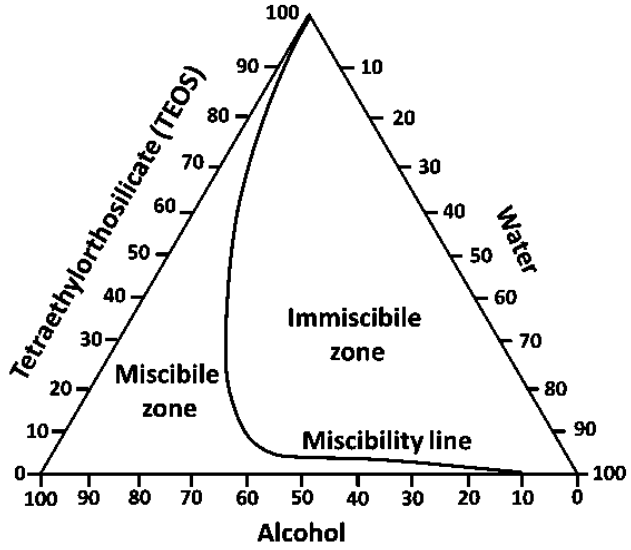

Fig. 2.7. TEOS-ethanol-water ternary phase diagram. Obviously the immiscibility increases with the increase of the content of TEOS due to the presence of hydrophobic ethoxy groups.[10]

2.1.5 Choice of the directing agent

The choice of the surfactant affects the pores diameter and distribution in mesoporous nanoparticles. Porous structure doesn't manifest itself for C_6 alkyl chain surfactant. The reason is due to the high solubility of short surfactant chains that tend to aggregate by restriction. It's also possible to use a mixture of directing agents and the average value of the pore diameters increases with the longer alkyl chain surfactant amount. In particular, it almost linearly increases with the increment of the number of carbons in the surfactant.[16] This aspect needs to be controlled in order to keep the pore diameter below a certain value that guarantee the amorphous form of the drug.
Moreover, BJH and TEM analysis by Beck et al. (1995) suggest that samples prepared by using alkyl chain length > C_{18} display regular hexagonal arrangement, that help a more uniform drug delivery, instead of an irregular or laminar ones. Under all these assumptions, we decided to use a quaternary ammonium surfactant, cetyltrimethylammonium bromide (CTAB, $C_{19}H_{42}BrN$, or $[(C_{16}H_{33})N(CH_3)_3]Br$).[5]

2.1.6 FITC and APTES

Nanoparticles in bioimaging play an important theranostic[1] role, being essential as facilitated cancer imaging application; using them, in fact, it's possible to track the loaded cargo of drug in both vitro and vivo samples. The most commonly used cell imaging technique is the confocal microscopy.
Fluorescence imaging requires fluorophores for microscopic visualization.[8] There's a very wide range of fluorescent compounds that can be used for this aim, depending on the available wavelength of excitation. However, due to photostability issues, organic probes aren't used as bare but in combination with nanoparticles, forming multifunctional materials, otherwise after thousand excitation cycles they would become photobleached.[18]
Contrast agents are used in conjugation with MSNs to track the entire biological processes involved in cancer treatment in real time under a dynamic point of view. Contrast agents or dyes can be both incorporated into the carrier matrix of the MSNs or adsorbed into the pores of MSNs, depending on limitations regarding aggregation. Dye-conjugated MSNs or fluorescently labelled-MSNs can be synthesized using either co-condensation or post-grafting. Both methods theoretically ensure the grafting of the inner pores as well as the outer surface, even if experiments have shown how the labelling after solvent extraction is more efficient.[20] In the co-condensation method the nanoparticles labelling is done during the synthesis, while post synthetic grafting employs MSNs surface modification after solvent extraction. Basically, taking advantage of the negatively charged SiO^- groups on both internal and external surface, resulting from deprotonation of surface silanol groups at neutral pH, through electrostatic interactions it is possible to attach positive charged moieties, such

[1] Theranostic is a new emerging field of medicine that unit diagnostic and therapeutic applications to form a single agent, allowing for diagnosis, drug delivering and live monitoring.

as dye.[19]

One of the most commonly used fluorescent dye is FITC (Fluorescein Isothiocyanate, $C_{21}H_{11}NO_5S$). The fluorescent properties of FITC include the maximum absorbance at about 495 nm and an emission wavelength of 520 nm.[22] This compound belongs to the class of organic compounds known as xanthanes; these are polycyclic aromatic compounds containing a xanthene moiety, which consists of two benzene rings joined to each other by a phyran ring.[21]

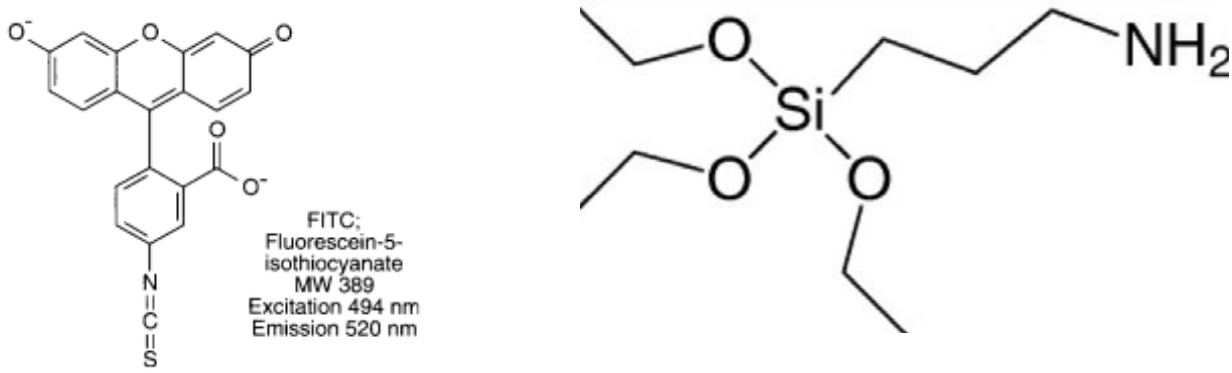

Fig. 2.8. (a) Chemical structure of FITC.[1] (b) Chemical structure of APTES.[58]

We have decided to introduce the organic functionalities through a single step synthesis, so with a co-condensation procedure, in order to avoid any pores blocking. Furthermore, in this way, FITC is more orderly distributed in the material comparing a post synthesis grafting procedure, even if with the second method a more hydrothermally stable material could be obtained[1]. The procedure is firstly carried out by reacting FITC with an organosilane, which is subsequently added in the co-condensation synthesis.

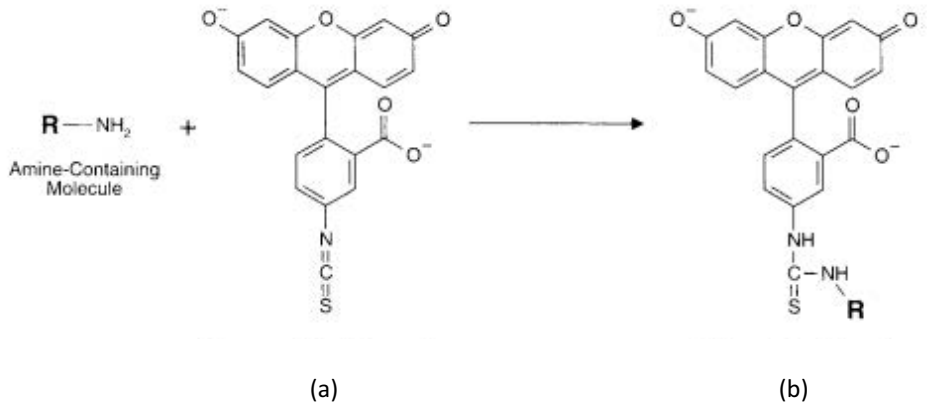

Fig. 2.9. (a) Fluorescein Isothiocyanate. (b) Thiourea Bond Formation.[1]

To produce fluorescent silica nanoparticles, we used APTES to bind FITC to the silica network through a Thiourea Bound.

The reaction between FITC and APTES involves the attack of the electrophilic carbon of the isothiocyanate group, to create a thiourea linkage, as can be seen in Figure 2.9.

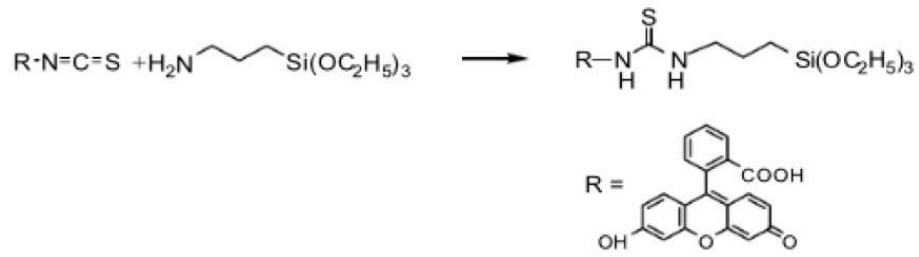

Fig. 2.10. FITC reacts with amine group of APTES.

Calling the ethyl group -C_2H_5 as R', APTES can be written as $H_2N(CH_2)_3Si(OR')_3$, while TEOS becomes $Si(OR')_4$. After the reaction between FITC and APTES, considering the group of aromatic rings of FITC as R (Fig. 2.9) and so that FITC becomes R-N=C=S, the obtained conjugated solution can be written as R-NH-C(=S)-NH-$Si(OR')_3$ (Fig. 2.10). For a further simplification, it can be written as R''-Si-$(OR')_3$.

Tab. 2.1. Formula of TEOS, APTES and FITC.

Substances	Formula	Formula in linear form	Simplified form
TEOS	$Si\ C_8\ H_{20}\ O_4$	$Si(OC_2H_5)_4$	$Si(OR')_4$
APTES	$C_9\ H_{23}\ NO_3\ Si$	$H_2N(CH_2)_3Si(OC_2H_5)_3$	$H_2N(CH_2)_3Si(OR')_3$
FITC	$C_{21}H_{11}NO_5S$		R-N=C=S

So, during the one step synthesis, the reaction between the tetraalkoxysilanes(TEOS), that's in the reaction solutions with CTAB, water, ethanol and NaOH, and the conjugated solution (R''-Si-$(OR')_3$), formed by FITC, APTES and ethanol, will rise to Si-C bounds. According to the illustration in Figure 2.11, at the end of the procedure, FITC, conjugated with APTES, is stuck on particles surface network.

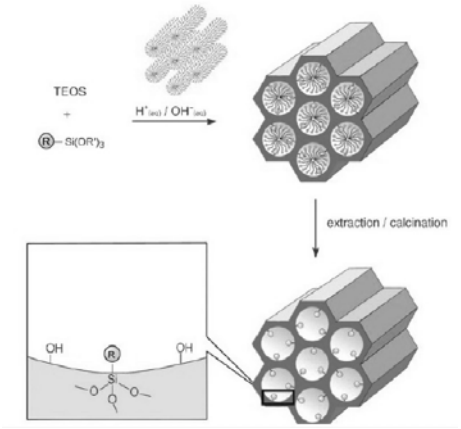

Fig. 2.11. Schematic final structure of labeled MCM – 41, that's a different nanomaterial but the result is the same.[1]

2.1.7 Choice of the temperature

A high reaction temperature can increase the rates of hydrolysis and polymerization of silica precursor, resulting in growth of the particles and formation of larger size MSNs. Moreover, temperature influences also the solubility of silica. Particles size increases upon increasing the reaction temperature from 40 °C to 95 °C.[14] Performing the synthesis at low temperature (T < 40°C), allows to form a large number of small and dispersed nanoparticles. Otherwise performing the reaction at temperature between 40°C and 95°C leads to bigger diameters but more monodispersability.[15]

We have decided to use a temperature of 33°C because 'big' size of the nanoparticles could imply clogging of nozzles used for printing, difficulties in cancer cell uptake due to the narrow blood vessels diameter and high temperature could cause instability of the dye (FITC). Photochemical instability of FITC constitutes an issue because when fluorescein isothiocyanate is heated more than 40°C, in the high pH (7-10) ambient in which we are working, has been proved that a considerable photobleaching takes place.[13]

2.1.8 Choice of the stirring velocity

The stirring velocity influences the particles size distribution. If the mixing is good enough an emulsion can be created, otherwise the two phases could stay separated. More is the stirring speed, more TEOS is in contact with the co-solvent-water mixture and this results in a hydrolysis acceleration and a quick reaching of the solution supersaturation. So, monodispersability of nanoparticles can be obtained increasing the stirring velocity.[15] The precise value depends upon the volume. Since it's not possible to state the right value a priori, until a microscopy analysis hasn't be done, in our case, to obtain an apparent homogeneous mixing, was selected speed control scale 2, that means 600 rpm[2].

2.1.9 Synthesis Procedure

MSNs were synthesized following a protocol based on a method described by Desai Diti et al. (2014) that complies with the project requirements. The detailed synthesis protocol was added in appendix 1.

Cetyltrimethylammonium bromide (CTAB) as structure-directing agent was dissolved in the aqueous reaction solution, followed by addition of sodium hydroxide (NaOH). After 30 minutes stirring, ethanol was added. Tetraethylorthosilicate (TEOS), as silica source, was added dropwise under hood

[2] Magnetic stirrer IKA C – MAG HS 7, Sigma Aldrich (USA).

at 33°C. The reaction solution was incubated under stirring at 33°C for 18 hours.[54] Fluorescent labelling of particles was led using fluorescein isothiocyanate (FITC). Pre-reaction of the dye with aminopropyltriethoxysilane (APTES) was carried out in 2mL of ethanol (Etax Aa) with a molar ratio (APTES:FITC) 1:3 and stirred for 2 hours under inert atmosphere. The pre-reaction, or conjugation, solution was added to the reaction solution right before the adding of TEOS to the synthesis.[54] The molar ratio between APTES and TEOS was varied from 1% to 10%. The final reaction was kept under stirring and under hood at control temperature (33°C) for 18 hours.

2.2 Mesoporous Silica Nanoparticles Extraction

The surfactant template can be removed from the mesoporous channels of the MSNs in order to make the network accessible for any surface functionalizations or simply to load cargo molecules, such as drugs.

2.2.1 Choice of the template removal technique

As evidenced by the wide number of sources about it, the commonly used method for template removal is the calcination. This technique includes a heat treatment, up to a temperature of 600°C, that removes all the surfactants since organic components burn at 200-300 °C.[25] However, it could cause contraction of the silica network, decrease of the pore size, collapse of the network and removal of amine groups that are useful for an eventual functionalization. Besides, this method is costly effective. To avoid severe damages of the structure after the template removal, many other different techniques have been investigated. Their efficiency depends on the interaction strength between the organic material and the inorganic framework. Plasma, ultrasound irradiations and ozone treatment[24], however, are methods whose efficiency has been proved, but due to their high cost-effectiveness and destroying effect on surfactant molecules, they have been discarded. For these reasons, solvent extraction seemed to be the most efficient way to remove the template, under the economical and final result perspectives. Another reason why we have chosen this method was due to the incorporation of FITC inside the nanosystem. In fact, the extraction procedure is the only one sensitive to the dye because it will not destroy its functionality.[1]
The main advantages that make this method even applicable for industrial scale are the minimization of structural damages and the low cost effectiveness.

2.2.2 Extraction Procedure

In recent years, many different solutions, such as hydrochloric acid (HCl), sodium chloride (NaCl), potassium chloride (KCl), sulfuric acid (H_2SO_4) and ammonium nitrate (NH_4NO_3) in ethanol have

shown to remove surfactant from silica nanoparticles.[24] The principal aim was to have an efficient and short operating time method. Chen et al. (2002) have proved that HCl/EtOH procedure is long time and detrimental for the network. The attempts to exchange surfactant molecules with Na^+ or K^+ cations have shown that more than 50% of the template still remains in the mesopores.[25] Furthermore, due to the high toxicity of H_2SO_4, we have decided to lead the extraction using 20% v/v solution of ammonium nitrate and ethanol. In this way, through ionic exchange between the surfactant and ethanol or extraction solvent, a free mesoporous network was obtained.

As we can notice from Figure 2.11, on the nanoparticles surface there are O_3SiOH groups. Interspersing several centrifugations and sonication steps, interactions between SiO^-, with which the template is associated, and NH_4^+ take place and the removal process is enhanced. Postponing to the sign + the species that are removed by the extraction, the procedure that takes place can be schematically summarized in that way:

$C_{19}H_{42}NBr$ (CTAB), $O_3SiOH \rightarrow C_{19}H_{42}N^+$ ($CTAB^+$), O_3SiO^-

$\downarrow NH_4^+$

NH_4^+, O_3SiO^- + $CTAB^+$ (Template removal)

$\downarrow$

O_3SiOH + NH_3 (Byproduct of solvent extraction)

Post the incubation period, the structure-directing agent was removed by washing the particles with 80 mL of NH_4NO_3. The dispersion was centrifugated (8000 rpm, 18°C) for 10 minutes after which the supernatant was removed and replaced by fresh extraction solvent. After 15 minutes ultra waves sonication simultaneously with vortexing, this cycle was repeated for a total of three times, after which it was possible to state that the surfactant molecules have been removed.[25] The last washing with pure ethanol (Etax Aa) was carried out to clear away any residues. The particles were then stored at +4°C. The same extraction procedure was followed for all the batches.

2.3 Mesoporous Silica Nanoparticles Characterization

Nanomaterial physicochemical properties greatly influence the biological behavior of the nanoparticles but are often challenging to measure and identify. In order to respect the Good Manufacturing Practice (GMP) and get the desired features, every stage during the nanomaterial fabrication or synthesis needs to be controlled. In fact, any variations in the manufacturing process or in the formulation may result in a generic product with different physiochemical properties such as size, size distribution and surface charge.

These physicochemical properties affect drug loading capacity, colloidal stability and interactions with loaded drugs, leading to a different biopharmaceutical profile with a significant impact on patient safety and therapeutic efficacy. Besides, these properties also affect nanoparticles toxicity.
The aim of this project was to develop a nanomedicine formulation, but since nanomedicines are NBCDs (Non Biological Complex Drug) because they are a complex medical compound (not just Active Pharmaceutical Ingredient), made in this case by drug-loaded MSNs, they cannot be characterized just by a 'simple' physiochemical analysis.[26] Before proceeding with the drug loading, the mesoporous structure, obtained after synthesis and solvent extraction procedure, needs to be investigated to evaluate if it shows all the desired features.
The resulting MSNs should show ordered mesoporous structure without interconnections between the channels.

We have characterized the MSNs using Dynamic Light Scattering (DLS), Zeta Potential (ζ- Potential) and Trasmission Electron Microscopy (TEM). Besides, in order to state the right amount of nanoparticles to dissolve in the printing ink, we evaluated the concentration of the five batches.
From previous studies[28] it was noticed that the properties of nanoparticles formulations depend strongly on surrounding medium. For instance, DLS becomes more complex than an aqueous medium, due to the presence of cells and proteins. Instead, Hepes buffer, used for Zeta Potential measurements, better simulates the body medium.

2.3.1 Dynamic Light Scattering

DLS it's used to characterize colloidal solutions and to find out the dispersity of the particles. By analyzing the modification of the scattered light intensity, that hits the sample after having been generated by a laser, as function of time, information about the hydrodynamic diameter can be obtained.

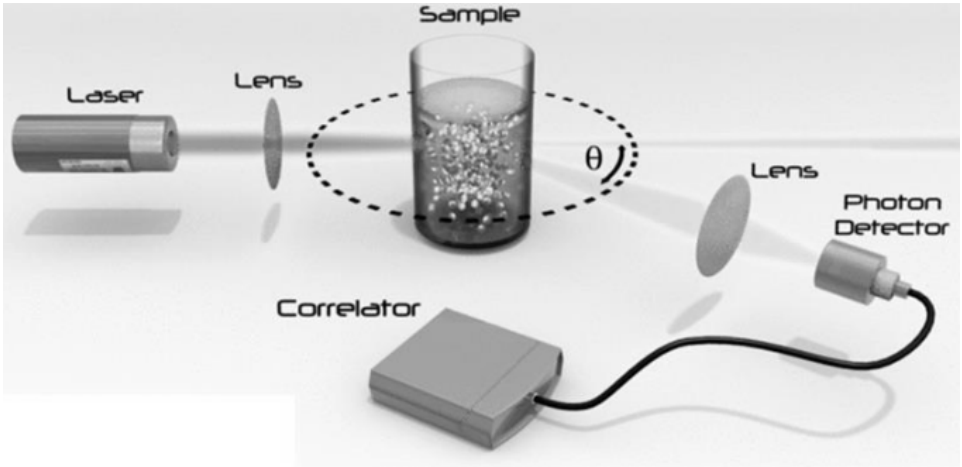

Fig. 2.12. DLS instrument.[62]

Since the high sensitivity of particles shape to the synthesis parameters, the porous particles are not all spherically equal, so each of them will move in a different way. The hydrodynamic diameter is a measure of the size of hypothetical hard, or non porous, sphere that diffuses in the same fashion as of the particle being measured, the porous one. The translational diffusion coefficient (D_t), to which irradiated nanoparticles are subjected, is correlated to the diffusion coefficient and it's calculated according to the Stokes-Einstein equation: $D = \frac{\mathrm{kB\ T}}{6\pi\eta R\mathrm{H}}$, where k_B is the Boltzmann's constant, T is the absolute temperature, η is the medium viscosity and R_H is the hydrodynamic radius. So, due to the Brownian motion, larger particles move more slowly and scatter less light compared to smaller ones. The indication of hydrodynamic diameter, in addition to particles size information obtained from a subsequent TEM analysis, provides information about the aggregation state of the nanoparticles. In fact, stable unaggregated colloidal solutions will have particles with hydrodynamic diameters similar to or slightly larger than their TEM size, while highly aggregated solution will have hydrodynamic diameters that are much larger than the TEM size.[27]

Another value that's important to check is the polydispersity index (PdI), that's the dimensionless measure of broadness of the size distribution calculated from cumulate analysis.

The measurements were done using the ZetaSizer NanoZS (Malvern Instruments Ltd., Worcestershire, United Kingdom). 100 µL of stored MSNs, after centrifugation (5 minutes, 9500 rpm), were separated by the solvent and dried for 10 minutes. The NPs were then dissolved in de-ionized water and sonicated for 15 minutes.

2.3.2 Zeta Potential

Zeta potential (ζ- Potential) is a physiochemical parameter of particular importance describing the effective charge on the particles surface and the stability of colloidal solutions, measuring the conductivity of an electrolyte solution. Very often it is used in combination with DLS in order to check the stability of the system and so the efficacy for cancer therapy[26], since agglomeration may involve clogging issues. The surface charge density of nanoparticles plays an important role in the way they interact with biological systems.

The ability to measure the surface charge density of nanoparticles in biological media is therefore of importance in understanding which would be the interactions between nanoparticles and proteins or drug.

Basically, when a charged nanoparticle is dispersed in a liquid, there will be an increase of concentration of ions of opposite charge on its surface. These ions will affect the distribution of other ions in the surrounding interfacial region, increasing counter-ions concentration close to the surface of the particle.[27]

Zeta potential is the measure of the difference in potential between the bulk fluid in which a particle is dispersed and the layer of fluid, containing the oppositely charged ions, that is associated with the nanoparticle surface. Zeta Potential is measured, using a conductivity meter (SI unit of measure is

siemens / meter), by determining the resistance of the solution between two flat of cylindrical electrodes separated by a fixed distance. The measure of the ability to conduct electricity by the colloidal suspension is done according to the Helmotz-Smoluchowski equation.

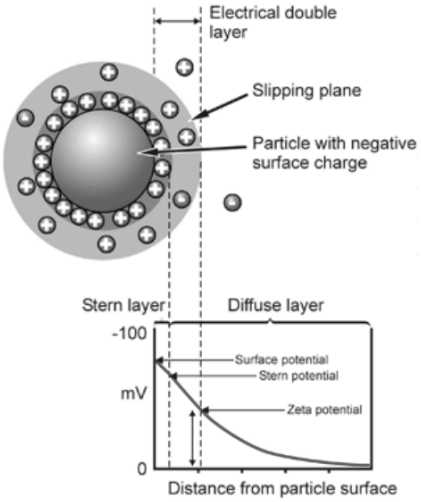

Fig. 2.13. Graphical representation of electrical double layer.[27]

Looking at Figure 2.13, the inner region (Stern layer) consists of strongly well bounded counter ions, while the outer layer (diffuse region) is formed by a cloud of electrical charges, less firmly attached. The potential 'closed' to the surface is called Zeta Potential and there's not a univocal definition for what 'closed' means.[1] The behavior of nanoparticles in the medium strongly depends on the Zeta Potential. Larger the value is, higher is the repulsion between the nanoparticles; this would avoid flocculation. Therefore, Zeta Potential should always be referred to a specific pH.

In the case of mesoporous silica nanoparticles, values are in the vicinity of 0 when pH is lower than 4, otherwise when the value increases from 4, the Zeta Potential becomes more and more negative, indicating that the negative charges on the particles surface have increased. Furthermore, nearby pH 2 or 3, Zeta Potential reaches the PZC, that is the pH value where positive charges on the surface perfectly balance negative ones.

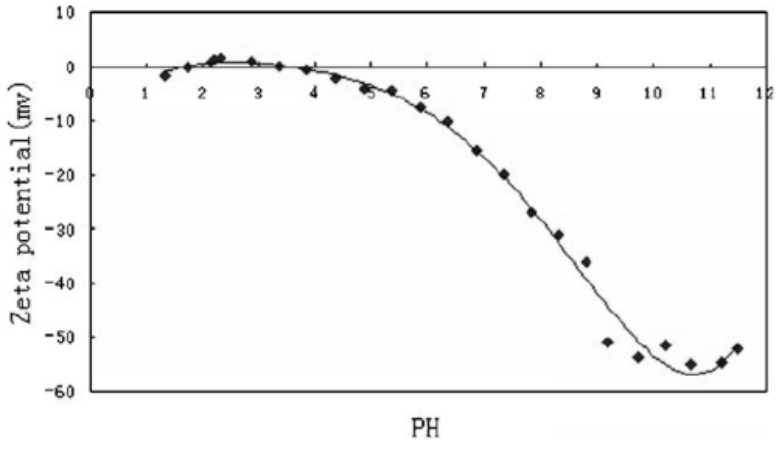

Fig. 2.14. Zeta Potential vs pH for MSNs.[30]

The charge of the MSNs surface depends on the choice of the catalyst. In fact, silanol groups formed on the internal and external mesoporous structure, depending on the pH of the media, could be catalyzed by a Louis base, such as NaOH, and the following reactions could happen, increasing the negative charge of the surface:

$SiO^- + H_2O \rightarrow Si - O - Si + OH^-$ $Si - OH + OH^- \rightarrow SiO^- + H_2O$

The evaluation of surface charge is also important to state if the functionalization has been done efficiently. In case of PEI coating (section 2.4.2) the surface modification increases the positive charge. The measurements were performed using the ZetaSizer NanoZS (Malvern Instruments Ltd., Worcestershire, United Kingdom). 100µL of stored MSNs, after centrifugation (5 minutes, 9500 rpm), were separated by the solvent and dried for 10 minutes. The NPs were then dissolved in HEPES pH 7.2 (99.5%, Sigma-Aldrich, Steinheim, Germany) and sonicated for 15 minutes.

2.3.3 TEM

To have a further better understanding of the particles morphology, porosity and size, we should combine DLS and transmission electron microscopy (TEM). TEM technique, however, is time consuming and often requires the sample in a dry state. Drying of nanoparticles increases the risk of changing the sample through shrinking or agglomeration and decreases the significance of the result. On the other hand, electron microscope analysis can find details that DLS cannot.[28]

TEM samples are either self-supported or mounted on a grid (copper grids are the most widely used). For nanoparticles, carbon film is used as support.

Using electrons instead of light, due to the smaller wavelength, a higher resolution compared to light-based imaging techniques can be obtained. A beam of electrons is transmitted through a sample and the imaging contrast, that is a function of the sample thickness (the amount of material that the electron beam must pass through) and the sample material, makes the structure visible. So, the image obtained is the bidimensional projection of the entire structure of the particle, not only of the top.[27]

Drying step during the sample preparation is of fundamental importance because it could cause accumulation and aggregation of nanoparticles, as well as liquid residual, resulting in a decrease of efficiency. Several underlying forces, i.e. Coffee Ring Effect, Marangoni flow, act during drying, producing overlapping projections or dark zones, in which the structure cannot be characterized. Colloidal interactions between MSNs are due to the presence of double layers surrounding the surfaces. The main attractive component is the Van der Walls interactions that increase accordingly with the drying, since the concentration of particles increases and the probability of collisions is higher. The result is the aggregation of nanoparticles. The disposition of nanoparticles on the grid depends upon wettability.[31]

10 µL of the colloidal sospension, previously sonicated (10 minutes), are piped inside an Eppendorf tube with 1 mL of acetone. After a further 10 minutes sonication, suspension is dropwise pipetted on

the TEM grid and let to dry at room T. Once the solvent has evaporated, the grid can be directly observed under the microscope.
TEM carbon fiber grids are usually coated with hydrophobic polymer films (Parlodium or Formvar).

2.3.4 Concentration

The determination of the concentration is a very crucial step because based on its value we can know how much is the drug, that needs to be used for the loading, and also the necessary amount of PEI for the surface functionalization. The concentration of MSNs was determined comparing the weight before and after centrifugation and drying. 100µL of stored MSNs, after centrifugation (5 minutes, 9500 rpm), was separated by the solvent, dried for 24 hours and then weighted.

2.3.5 Thermogravimetric Analysis

To examine the efficiency of PEI surface modification of 1% APTES-FITC MSNs, as well as Zeta Potential, we used a thermogravimetric analysis (QMS 403 C Aëolos Quadro, NETZSCH, Selb, Germany). The measurement was performed on an aluminum oxide vessel, containing 7.28 mg (AT261 DeltaRange Professional Analytic Balance, METTLER TOLEDO, Columbus, USA) of PEI coated MSNs; the mass variation of the sample was measured over time as the temperature constantly increased (STA 449 F1 Jupiter, NETZSCH, Selb, Germany) with a 10 K/minute rate from 30°C to 900 °C.

2.3.6 Nitrogen Adsorption

Nitrogen adsorption is one of the most important method of characterization of porous materials. Evaluating the change of nitrogen pressure, the resulting amount of gas adsorbed leads to determine the values of pore volume, pore width and surface area. According to the theory implemented, the results can be different. For surface area determination we used the BET method. This theory assumes that lateral interaction between gas molecules adsorbed, on a fictitious array characterized by a uniform pores size distribution, are not allowed. Instead, to determine the pore width and the pore volume, we used the density functional formulation, which explores them as regular cylinder pores which are assumed to behave independently from the neighbors.[49]
The nitrogen adsorption procedure starts with an initial degassing that's mainly done to remove the still adsorbed species from the sample, otherwise the presence of them, i.e. moisture, could negatively interact with the formation of N_2 layers on the surface, making the surface area measurement inaccurate. The choice of degassing temperature is related to the thermal stability of material under investigation and since we were working with fluorescent samples, we decided to use 50°C.

Even the degassing duration is important to guarantee a complete drying. If it's stopped before being completed, an increase of pressure due to evaporation of water still present will be perceived by the machine. PEI MSNs were degassed for 20 hours.[63]
The measurement was performed using Autosorb-1 (Quantachrome instruments, Boynton Beach, FL, USA).

2.4. MSNs Surface Functionalization

The use of silica nanoparticles as complex drug delivery nanosystem is improved by the ease with which it is possible to obtain tunable sizes, that as previously said make them absorbable by the cells, stable frameworks compared to other carriers and uniform and narrow pores size distribution. However, one of the main challenges for MSNs efficacy is the presence of the reticuloendothelial system (RES), that is a network of cells located throughout the body that help filter out foreign materials, i.e. nanoparticles, in both blood and tissues, consequently causing a low drug delivery efficacy to the targeting tissue. Most of the nanoparticles are recognized and removed by RES of the liver and spleen.[32]
Another issue toward the application of these particles for clinical purposes is the colloidal instability of the carrier, that could lead to agglomeration in the circulation and may therefore lead to decrease the enhanced permeability and retention (EPR) effect[3].
In order to reduce the interactions with the immune system, the strategy we have adopted is the surface functionalization.[18] Surface functionalization of nanoparticles, in fact, enhances both internalization by cancer cells and intracellular drug delivery; moreover, it allows live cells imaging, coating the surface with fluorescent dyes, such as Fluorescein Isothiocyanate (FITC).
The surface functionalization design depends on the specific aim; in particular, the attachment of affinity ligands or antibodies could promote the recognition of cancer cells, while the polymeric coating could be used to reach longer circulation time of the nanocarriers inside the body, colloidal stability and good cell internalization.
Surface functionalization made by the so called 'smart polymers' allows to control drug release through endogenous or exogenous methods, that could be both dual or multi responsive, acting as 'smart gatekeeers'.[1]
Basically, the release of drug can be manipulated by changing the properties of the polymers, for instance, by pH or thermal stimuli; or the drug can be conjugated with the polymer using a linker that can break down in presence of a stimuli when it reaches a target side of the body (for instance reaching the tumor tissue, where pH is 0.5-1 units lower than the pH value of the healthy surrounding, due to metabolic glycolysis and lactic acid production).[3]

[3] EPR effect: Enhanced Permeability and Retention effect, concept by which nanoparticles tend to preferably accumulate in tumor tissues instead of normal healthy tissues.

2.4.1 Methods

There are three different surface modification procedures that can be implemented: co-condensation, post-synthesis functionalization and physical coating.
In the co-condensation, the silane coupling agent and TEOS are co-condensed during the synthesis, obtaining organic moieties both internally and externally attached.
The post-synthesis functionalization employs a chemical modification of accessible silanol groups inside the mesoporous network and on the external surface. While, the physical coating is carried out ,as the previous one, after synthesis and surfactant removal, but through noncovalent electrostatic interactions between the surface and the linkers. So, these last two techniques are post synthesis modifications. The introduction of the dye by a post-grafting method consists in a chemical conjugation process, called grafting. This physical coating can be both 'grafting from' or 'grafting to'.[1] The first one employs to initiate from the surface polymers, while the second one means leading a reaction between surface groups with compatible groups. Hence, the 'grafting to' could result in a low groups density on the surface because of steric hindrance with groups previously attached, such as dyes.

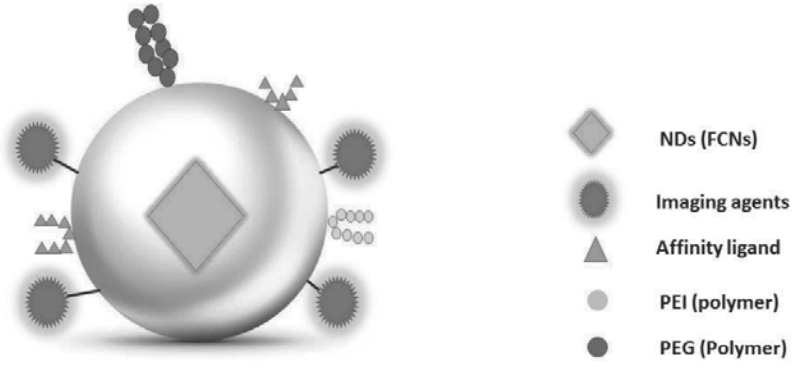

Fig. 2.15. Various linkers to attach to modify MSP properties.[18]

Generally, the structure of the carrier is retained, even if an inhomogeneous distribution of functional groups may result because of high density of organosilanes grafting on the surface, that could cause pores clogging and a non complete internal surface functionalization. Number and accessibility of silanol groups are determinant for the functionalization.[2]
Also the presence of water could lead to undesired reactions between organosilanes and water, causing polymerization, that we need to avoid to preserve the porous structure; for that reason the drying has to be done properly.

2.4.2 PEI grafting

E. Frölich (2012) has shown how the positive charge, due to the PEI coating, enhances the affinity for interactions between nanoparticles and cell membrane, increasing the cellular uptake. Moreover,

it has been demonstrated that interactions between neutral NPs or those bearing negative charges and the negatively charged lipid bilayer is weaker compared to those ones with positive charges.[34]

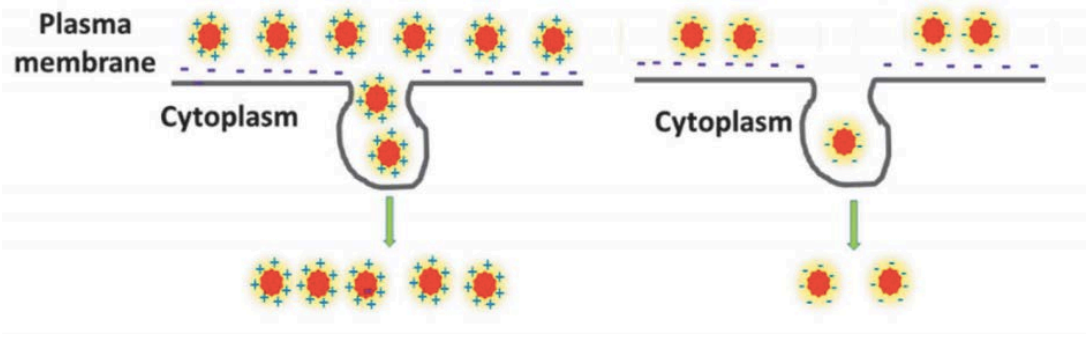

Fig. 2.16. Representation between positive and negative charged NPs with the lipid bilayer.

So, based on the literature, we decided to PEI functionalize NPs in order to enhance the uptake by the cancer cells and to take advantage from this cationic strong electrostatic repulsion to inhibiting the particles aggregation, achieving stable dispersion of MSNs.[32,37]

2.4.3 Reactions and steps involved

MSNs were surface functionalized with Poly(ethyleneimine) (PEI). Ammine groups (NH_2) and silanol groups (SiOH), present on the surface, can initiate the polymerization of aziridine (Menadiona, Barcelona, Spain), giving rise to a PEI layer, whose thickness can be simply modified changing the aziridine/silica ratio.[35] As we can see from Figure 2.17, both groups directly react with aziridine, catalyzed by acetic acid (99%, Sigma-Aldrich, Steinheim, Germany) as catalyst, resulting in a hyperbranched polymer.

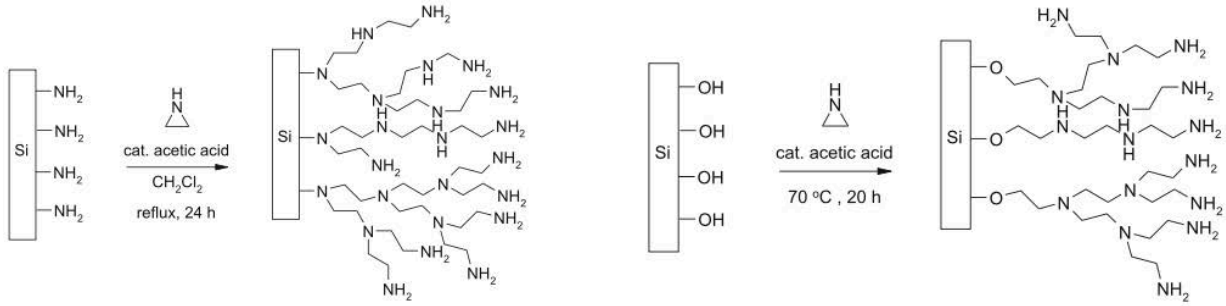

(a) (b)

Fig. 2.17. (a) PEI growing from ammino group. (b)PEI growing from silanol group.

Surface polymerization was performed with toluene (99.8%, Sigma-Aldrich, Steinheim, Germany) as solvent, in which the substrates were suspended after being carefully vacuum-dried and sealed under vacuum and subsequently subjected to inert atmosphere.

480 mg of 1% APTES-FITC MSNs were collected for the PEI functionalization. Many studies[35] led before have proved grafting efficiency creating a 10 mg/mL solution of NPs in toluene.

The adding of toluene has been done in two steps; the first one has involved 30 mL, the second one 20 mL, to obtain 10 mg/mL concentration, as suggested. These two moments were interspersed by 10 minutes sonication and 5 minutes stirring. In the case of bare nanoparticles, to obtain an effective ring opening polymerization on the surface, the suspension could be refluxed under inert atmosphere at 75°C during the PEI functionalization.[36] But, in presence of FITC, due to photostability issues, as mentioned earlier in section 2.1.6, a temperature of 30°C has been used, followed by the addition of 26 μL of acetic acid and 260 μL of azidrine, and allowing the solution for overnight stirring, approximately 18 hours. The extraction procedure was done in two teflon Nalgene tubes containing 25 mL of the solution by a 10 minutes centrifugation, at 8000 rpm and 15°C, in order to remove the toluene, which could cause toxicity issues. After having dispersed again the nanoparticles in 30 mL of ethanol per each tubes, another centrifugation with the same parameters took place to wash out the toluene. The final grafting particles, were dispersed in ethanol again and subjected to characterization. The efficiency of the polymerization depends on the solvent; it was observed that dichlorometane and toluene are the most successful ones. In particular, we chose to use toluene to obtain a smoother polymerized surface than that one got with dichloromethane. Moreover, the resulting organic layer shows high thermal and pH stability, which reconfirms covalent bond formation between the silanol and aziridine.[36] However, polymers of 10kD or less still promote cells uptake, although they make the particles cytotoxic.[37]

2.5 Ink Development

Propylene glycol (≥ 99.5, FCC, FG,Sigma Aldrich Corporation, USA) (PG), isopropanol (Propan-2-ol, Fischer Chemical, USA) (IPA) and de-ionized water (Milli-Q water, Millipore Corporation, USA) (MQ) were combined in different volume ratio to figure out the proper inkbase formulation.

2.5.1 Ink Formulation

For a successful printing, the ink physical properties such as the printer parameters needed to be well optimized. A pharmaceutical ink made up of mesoporous silica nanoparticles was developed after having tested several different formulations to ensure fluid stability and accuracy after printing. The quality of the single droplet ejected was firstly evaluated for the ink base and, after having optimized the settings, the same procedure was adopted for polyethyleneimine surface-functionalized MSNs dispersed in the ink (concentrations of 0.1, 0.5, 1 and 5 mg/mL).
MSNs are usually studied in an aqueous ink because its similar behavior to biological media.[45] However, the choice of the ink chemicals needs to be done according to the specific drug under

investigation in order to avoid its solubilization inside the fluid. This could cause drug leaching during the processing step, making the therapeutic aim of nanoparticles ineffective.
Viscosity, surface tension and density of the ink are the most crucial aspect of the ink-jet printing. PG was added as ink excipient in order to decrease the surface tension of water (72 dynes/cm, at 25°C). Due to the cohesive nature of molecules forming water, it would exhibit a strong resistance to the external forces generated in the ink-jet printer, preventing the formation of droplets. However, the surface tension should be maintained sufficiently high (25-45 dynes/cm, at 25°C) to guarantee the droplet formation. Moreover, it was also used to increase the viscosity of the ink, to respect the ink viscosity indications provided by the manufacturer (8-20 mPas), since a lower viscosity than that one recommended could involve long refilling time of the nozzles and tailing generation followed by satellite droplet formation.[44]

2.5.2 Printing

A piezoelectric Drop on Demand printer was used to print a designed pattern made by 24 cardboard circles (8mm diameter) that resembles the Petri dishes , that thereafter biologists would use to test the printed product efficacy. The inkjet printer used was the PixDroLP 50 (OTB Solar – Roth & Rau, The Netherlands), with the printer head Spectra SL748, equipped with 128 nozzles of 50 µm diameter. To ensure a complete wetting of the circles, firstly we decided to print on a 35 x 105 mm rectangular and the hydrophobic and hydrophilic subdivision of the substrate resulted in different contact angle. However, the chaotic distribution of nanoparticles, got from fluorescent microscopy analysis, suggested to respect the printing pattern proposed. Printing was performed by imposing a QF=2, where QF determines the number of nozzles that should print a line.

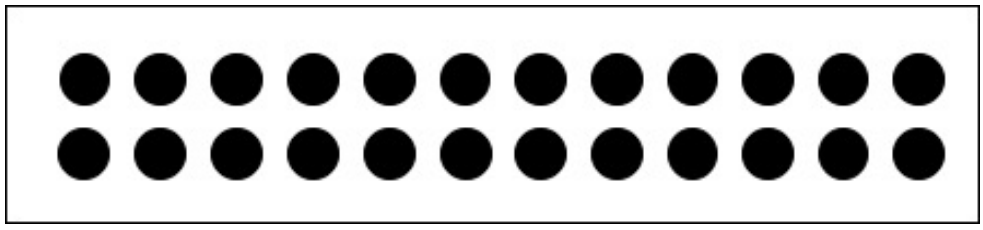

Fig. 2.18. Printing pattern. The space between each circle is 0.4 cm, the distance from the top is 0.75 cm, from the left side 0.85 cm, from the right 0.5.

2.6 Ink Characterization

Based on previous studies[43] a good positioning accuracy for the pattern could be obtained for Z values between 5 and 9. To define the Z value, several ink formulations were characterized.

2.6.1 Viscosity

Rheological properties of the fluid were investigated with a rotational rheometer (Physica MCR 300, Anton Paar, Graz, Austria, Software: Rheoplus), equipped with a coaxial double gap geometry (DG26.7/T200/SS, diameter internal: 24.655 mm, diameter external: 26.669 mm). The dynamic viscosity of the blank and of the colloidal suspensions in the ink were measured at 22 $\pm$ 0.5 °C, applying a 10 s^{-1} shear rate ramp, from 0.1 to 3000 1/s, to monitor the behavior of ink at printing operating values.

2.6.2 Surface Tension and Contact Angle

The modular optical contact angle and surface tension meter CAM 200 (KSV Instruments Ltd., Espoo, Finland, later Biolin Scientific) was used to perform dynamic measurements of contact angle and surface tension of liquids. These surface characterizations were done at room temperature (32.9 °C), dispensing a 5μL drop from a plastic tip (Fintip 200 μL, Thermo Scientific, Vantaa, Finland) and video capturing the images for 10 seconds. The automatic baseline images analysis for both surface tension and contact angle was performed based on the Young-Laplace equation using the One Attension software. Adjusting the drop size (μL) and rate (μL/s) according to several samples, to determine the surface tension and the contact angle, the pendant droplet and the sessile drop methods were respectively implemented.

2.6.3 Density

The density of the ink formulations, with and without nanoparticles, was measured weighting 1mL of the samples, at room temperature (32°C).

2.6.4 Confocal Laser Scanning Microscopy

The prints were imaged using Microscope Leica TCS SP5 8 (Leica Microsystems, Wetzlar, Germany) and the Leica Application Suite Advanced Fluorescence. The number of pixels was set on 1024 x 1024, the frequency on 400 Hz, and the excitation wavelength ranged between 510 and 550 nm. It

works on the principle of excitation of the fluorescent dyes (FITC), which resulting signal is channeled towards a pinhole and detected by an image detector. A smaller beam of light, produce by a second pinhole, is focused at one depth level at time and since not the whole specimen is investigated, only the light produced by fluorescence near to the focal plane can be detected. The optical resolution is better than a conventional fluorescence microscopy instrument because the disturbs due to the diffused light from unfocused parts of the sample are eliminated.

2.6.5 UV – Vis Spectroscopy Analysis

UV- Vis (NanoDrop 2000c spectrophotometer, Thermo Fisher Scientific, USA) is a technique that is used to quantify the light that is absorbed and scattered by a sample. Generally, performing analysis from 200 to 1100 nm and comparing the values of intensity of the light passing through the sample (I) and before passing (I_0), so the transmittance (I/I_0), the value of absorbance is obtained.
Besides, the ratio between the light that is scattered by the sample and that one reflected from a reference material determines the reflectance.[27]

2.7 Drug

Nanoparticles were loaded with PF-3084014 (Nirogacestat), $C_{27}H_{41}F_2N_5O$, which was purchased from MedChemExpress (USA). In vivo studies on mice showed robust antitumor activity, underlining also that tumor growth inhibition is dose dependent.[18]

2.6.1 Drug Formulation

PEI MSNs were used as drug delivery vehicles for nirogacestat, that has shown poor solubility, to facilitate target delivery and to induce the cancer cells death.[14] During the drug loading, the polymorph or the crystal form of the drug should always be monitored in order to state if phase transformations occur. Recrystallization of the drug during the storage, due to the thermodynamic instability of the system (heat, moisture, mechanical stress), could affect its performance and stability. The crystallization inhibition is imperative to maintain the therapy efficiency[15], as has been proved in many other references concerning other drugs. Generally, only amorphous metastable forms of the drugs guarantee higher solubility and faster dissolution rate.[16] However, the almost impossibility to recover drug related information, due to the fact that it is an unknown drug whose just clinical efficacy has been proved, makes difficult to predict a priori the interactions between the API and MSNs, that impact on the drug form.

Drug loaded nanoparticles can be analyzed using a wide variety of techniques and, during studies previously done, X-ray diffraction analysis has proved that ordered mesoporous silicates are not structurally affected by the loading and the drug is not arranged in crystalline form.[17] Considering that the pore size is slightly higher than the longest drug dimension, confining it inside nanospaces, crystallization is prevented.

2.6.2 Drug Loading

The drug loading was carried out through the solvent immersion method. Drug loaded MSNs were used both for testing the drug leaching and for printing. The process involved the dispersion of 5 wt% of drug with respect to 1% APTES-FITC PEI MSNs in cyclohexane (anhydrous, 99.5%, Sigma Aldrich Corporation, USA). The suspension was sonicated for 15 minutes and kept rotating over night for 18 hours. The loaded MSNs were studied in the ink base to ensure that no premature drug leakage happened during the manufacturing steps.

2.6.3 Drug Leaching in ink

To be sure that not premature drug leaching during the printing process took place, drug release from MSNs in the ink formulation was monitored running the rotor (Hei-TORQUE, overhead stirrers, Heidolph Instruments GmbH&CO, Germany) at 65 rpm for 3 and 5 hours.

3. RESULTS

3.1 MSNs Characterization

3.1.1 Size distribution and Zeta Potential of MSNs

The MSNs size distribution was evaluated by Dynamic Light Scattering (DLS). DLS was used to evaluate the hydrodynamic diameter of MSNs and their dispersity both in water and ink. The measurements were performed three times for each sample synthesized, as earlier mentioned in section 1.3.

Figure 3.1 shows the size distribution of 1% APTES-FITC MSNs in water. The average particle size, at 25°C, was 636.5± 130.3 nm, with 0.271 as polydispersity index. The peaks are centered on one value, meaning no aggregates are present.

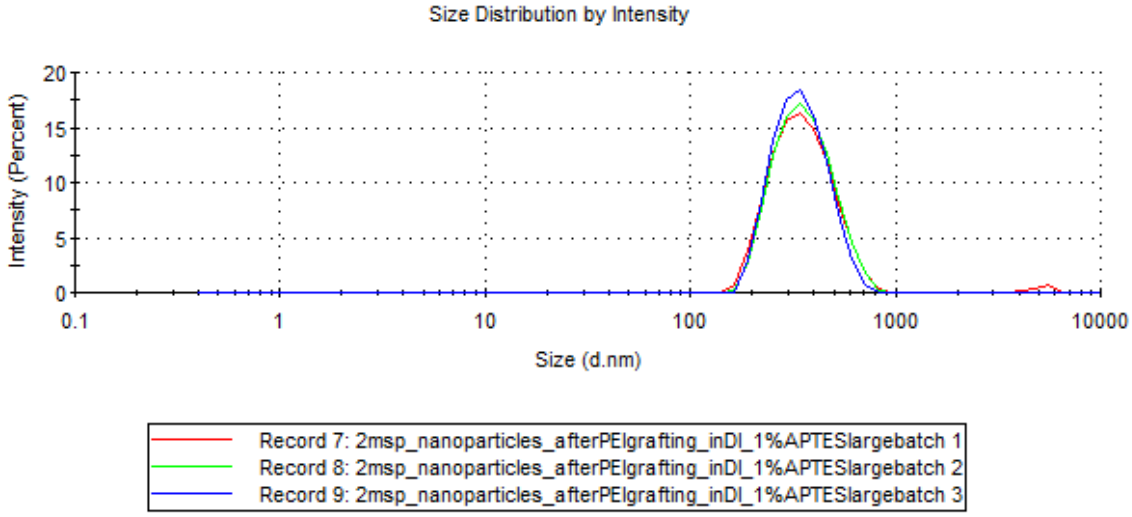

Fig. 3.1 Size distribution of 1% APTES-FITC MSNs PEI functionalized in water.

The size distribution was also assessed for unloaded 1% APTES-FITC MSNs inside the ink formulation[4] (1 mg/mL). The average particle size, at 25°C, was 586.3± 24.6 nm, with 0.048 as polydispersity index (Figure 3.2).

[4] Refer to section 3.3.

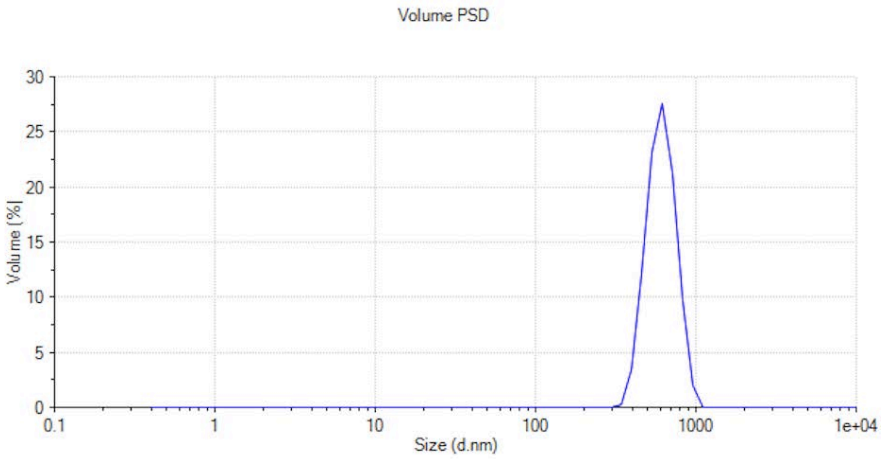

Fig. 3.2. Size distribution of unloaded 1% FITC-APTES MSNs PEI functionalized in ink formulation.

To evaluate stability of MSNs, Zeta Potential was measured. The measurements were performed in Hepes buffer (99.5%, Sigma-Aldrich, Steinheim, Germany), that is a solvent of known pH (7.2), so based on Figure 2.14, a value of Zeta Potential between -10 and -20 mV should be obtained.

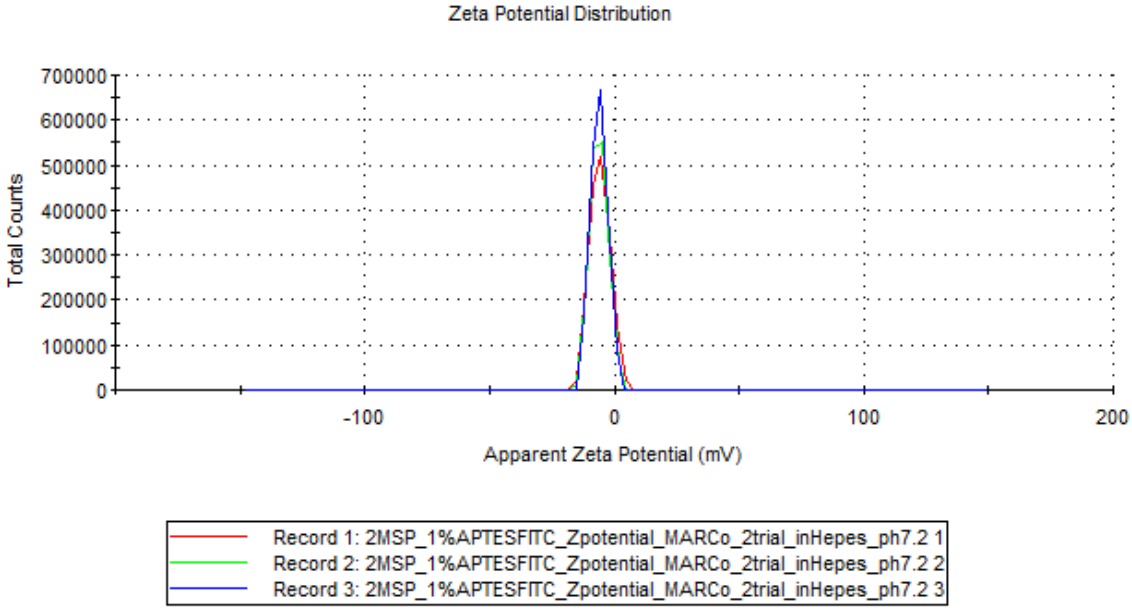

Fig. 3.3 Zeta Potential Distribution of unloaded 1% FITC-APTES MSNs.

As we can see from Figure 3.3, at 25°C, Zeta Potential was equal to -5.97 $\pm$ 0.25 mV, with a conductivity of 0.634 $\pm$ 0.01 mS/cm.

The obtained value of Zeta Potential can be used to state whether the surface functionalization has been successfully carried out. As previously said in section 2.3.2, PEI coating should positively affect the surface charge of MSNs. In fact, at 25°C, Zeta Potential of PEI functionalized MSNs was equal to +27.9 $\pm$ 0.737 mV (Figure 3.4), with a conductivity of 0.603 $\pm$ 0.01 mS/cm.

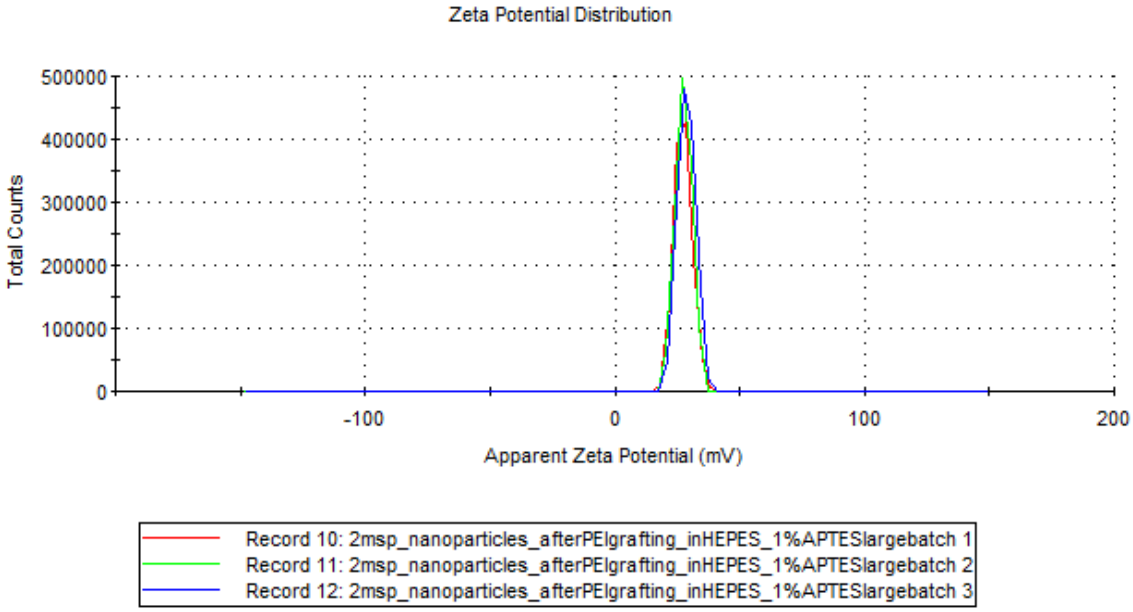

Fig. 3.4 Zeta Potential Distribution of unloaded 1% FITC-APTES MSNs PEI functionalized.

3.1.2 Effectiveness of surface functionalization

The TGA-DSC curve (Figure 3.5), provided by the software, plotted on the left y-axis the percentage decrease of the initial mass of the sample, that was exposed to a costant heating, and on the right y-axis curve of the heat flux (µV/mg), both of them versus temperature (°C).

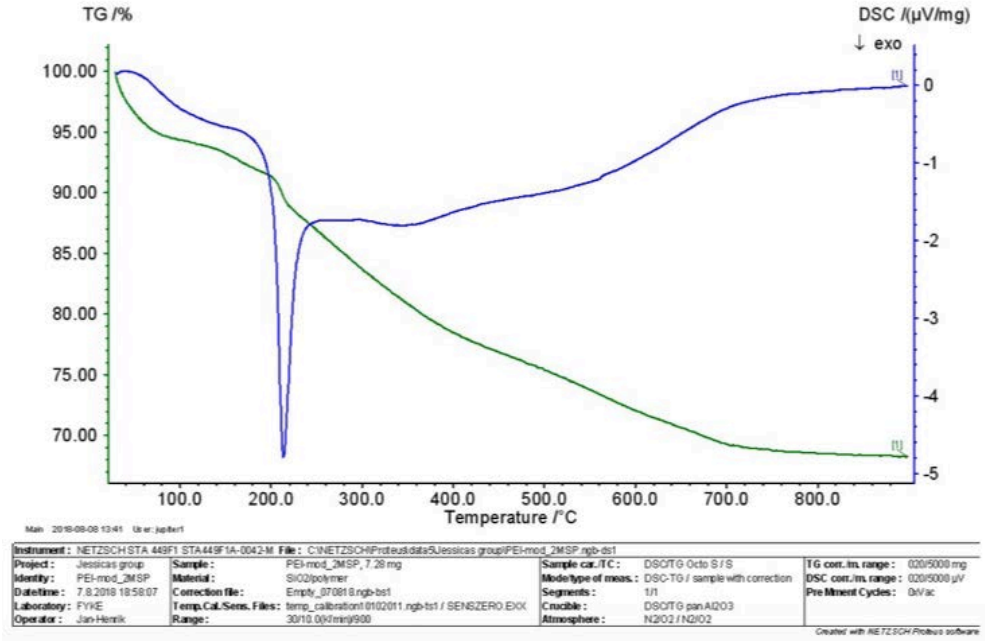

Fig. 3.5. Thermogravimetric Analysis of 1% APTES-FITC MSNs PEI functionalized

At the final point of the curve the residue value was 68%, equal to 4.95 mg, of the initial mass (7.28 mg). At 210°C material exothermic degradation occurred, sign of thermal instability. The mass change observed was due to combustion of PEI, since its flash point is closed to 220°C.[52] DSC trend shows an exothermic reaction that affects a wide temperature range, meaning that other reactions took place, such as evaporation of water, moisture or template, that the extraction procedure didn't entirely remove.

Due to the decomposition of both PEI and residual CTAB, at 200°C a slope increment occured.[53] So, even if this technique didn't provide a straightforward value of PEI grafting, since more than one chemicals took part in the combustion process, TGA revealed that the amount of PEI grafted on the surface approximately was 16 wt%, since after its flash point temperature there's a decrease of mass that graphically can be quantified as 16 wt%.

3.1.3 Transmission Electron Microscopy of MSNs and concentration

The aim of this study was to check if the nanoparticles were spherical and if they had a radial pores distribution. Besides, it was also important to evaluate the efficiency of the extraction procedure. Although the darkness in the middle, due to drying inefficiency that causes interaction between the residue liquid and TEM electrons, prevents to carry out a detailed analysis of MSNs structure, distribution of the pores in Figure 3.6 seemed to be more radial than in Figure 3.7.

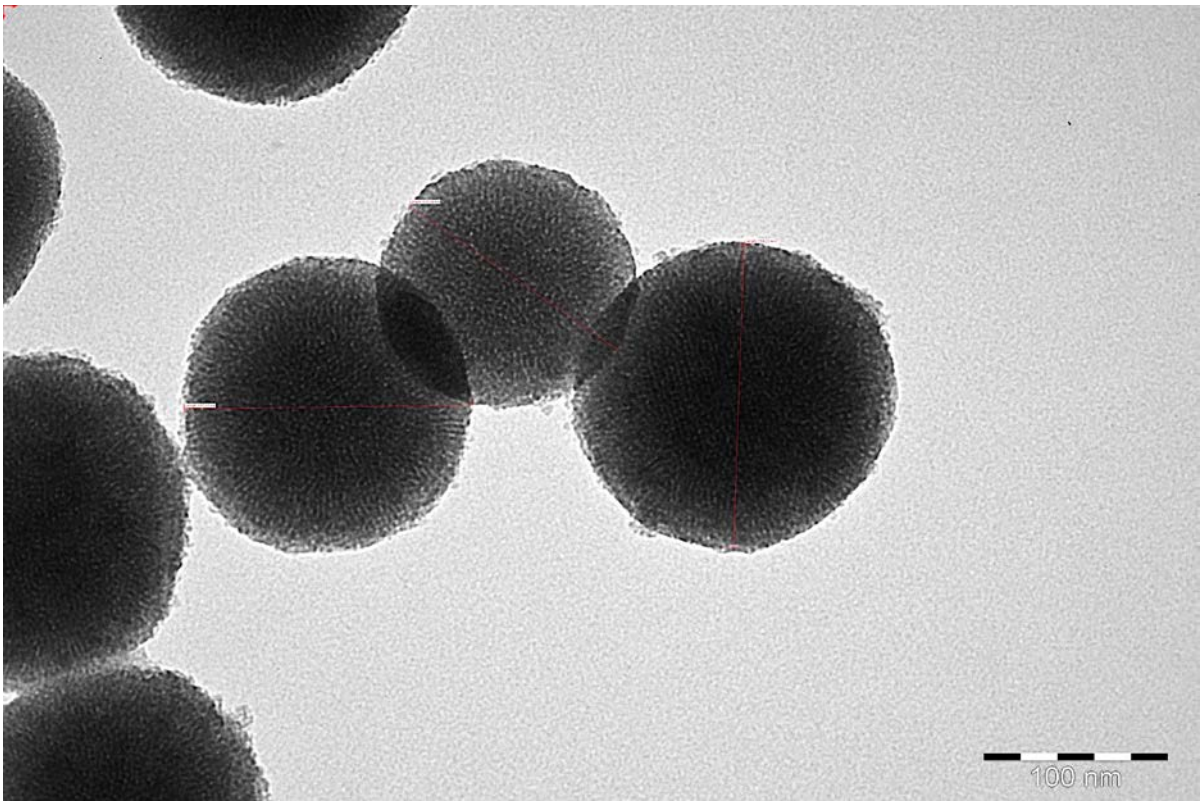

Fig. 3.6. Unfunctionalized 1% APTES -FITC MSNs (400 mL).

Both samples refer to 1% APTES-FITC, synthesized for different volume, as earlier mentioned in 1.3 section.

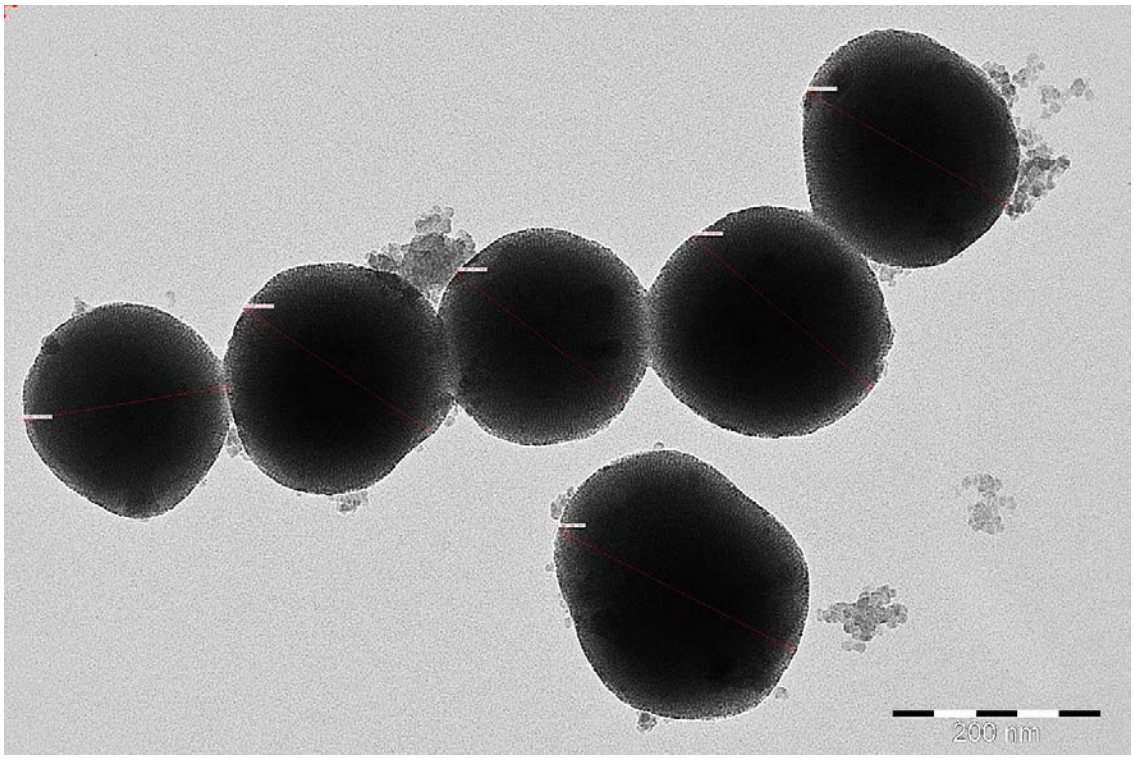

Fig. 3.7. Unfunctionalized 1% APTES-FITC MSNs.

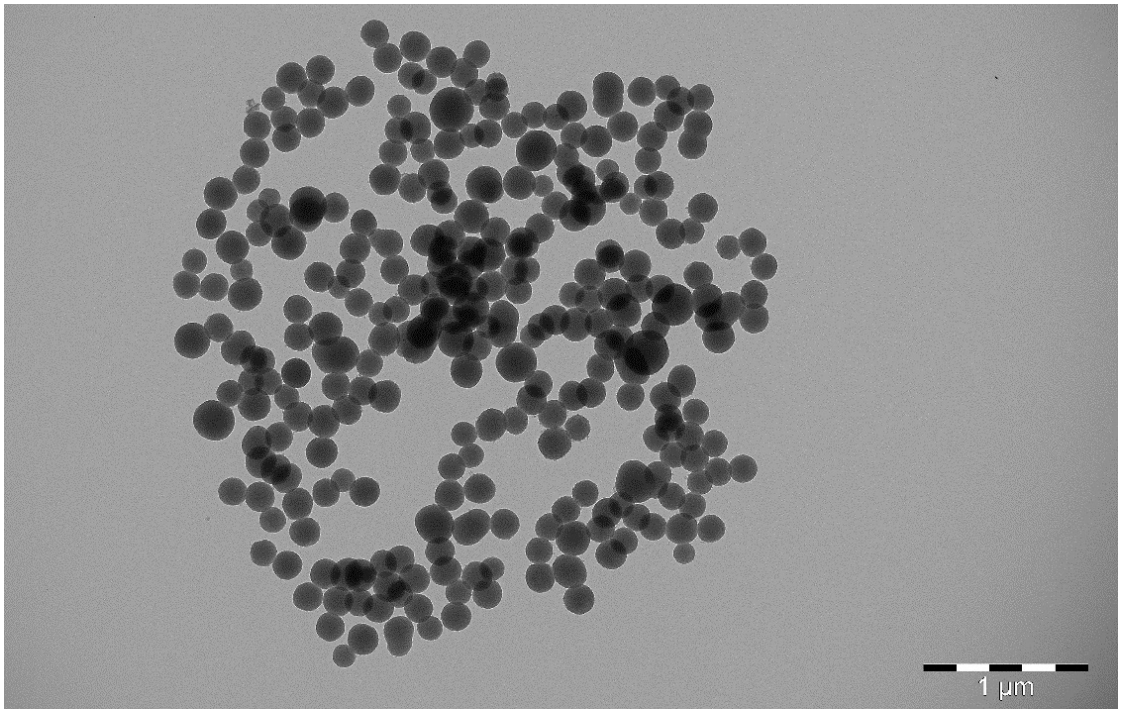

Fig. 3.8. Unfunctionalized 1% APTES-FITC MSNs.

Randomly choosing the particles to check, three different diameter values were obtained: 164.72 nm, 157.17 nm and 137.89 nm. Anyway, though it's not possible to state that certainly all the particles size were in this range, we can say that it is less than 180 nm with a 1% margin of error.

The concentration of MSNs was determined for all the batches synthesized:

Tab. 3.1. Concentration of MSNs.

Batch	Difference [mg]	Concentration [mg/100 µL]	Concentration [mg/mL]
MSNs	1194.7 – 1192.1	2.6	26
1% APTES-FITC MSNs	1189.5 – 1188.5	1.0	10
1% APTES-FITC MSNs (400 mL)	1192.2 – 1190.0	2.2	22
5% APTES-FITC MSNs	1193.4 – 1192.0	1.4	14
10% APTES-FITC MSNs	1195.1 – 1193.3	1.8	18

3.2 Drug Analysis

3.2.1 Uv-Vis Analysis

The wavelength absorbance of the drug was tested for 1 mg/mL solution, in acetonitrile (HPLC grade, ≥ 99.93 %, Sigma-Aldrich). Collecting Uv-Vis analysis spectra from 220 nm to 248 nm, three discernible peaks were identified respectively at 230, 244 and 248 nm. The optimal wavelength used for baseline correction was set at 340 nm, since for methods that use UV ranges between 190 and 350 nm it ensures no absorbance attributed to the sample buffer or the molecules of interest.[9]

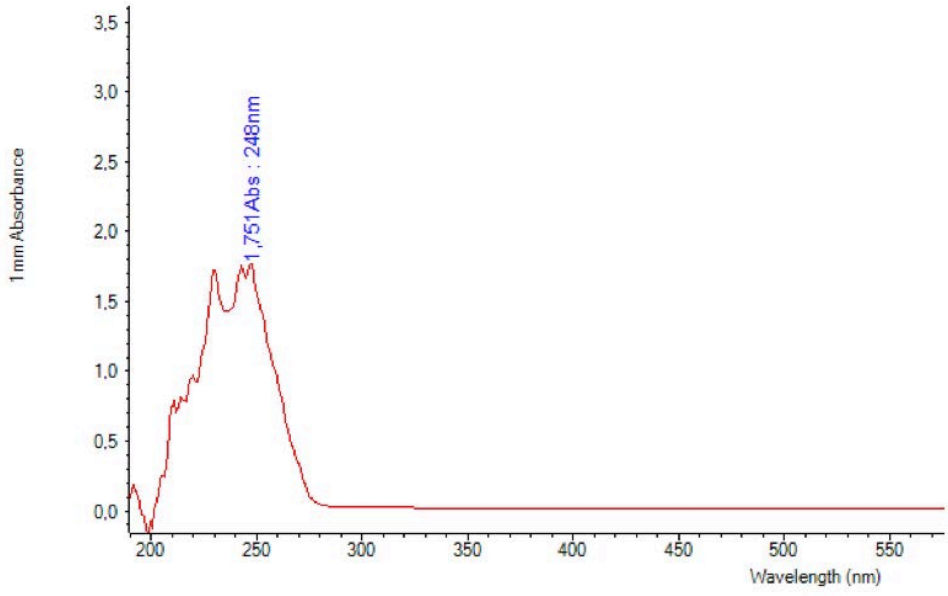

Fig. 3.9. Nirogacestat absorbance spectrum in acetonitrile.

A further analysis dissolving the drug in methanol (HPLC gradient grade, J.T. Baker, Center Valley, USA) (1.2 mg/mL) provided a straightforward indication about the wavelength absorbance. As can be noticed from the Figure below, the absorbance wavelength of the drug can be identified at 248 nm.

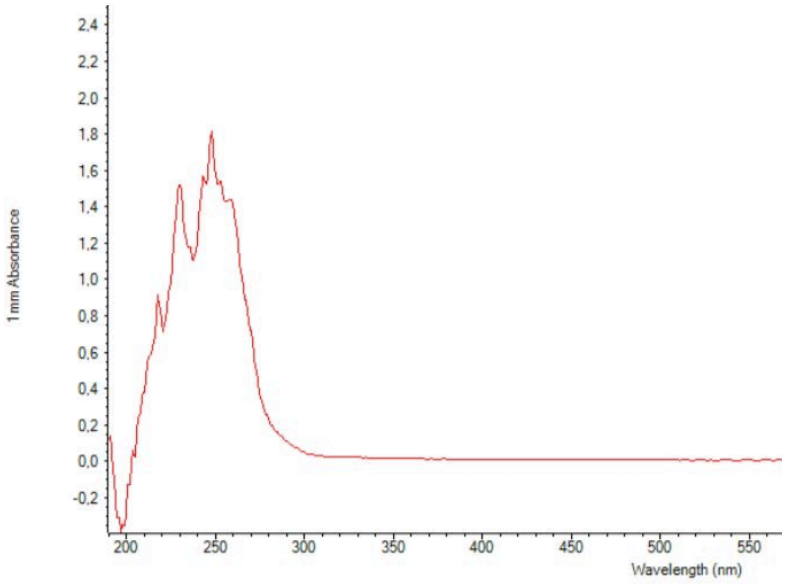

Fig. 3.10. Nirogacestat absorbance spectrum in methanol.

3.2.2 Nirogacestat calibration curve

The standard curve (Figure 3.11) allows to determine the concentration of drug leached in an unknown sample by comparing the unknown to a set of samples of known concentration. This allow to quantify, after printing, the dose of drug still present inside nanoparticles.

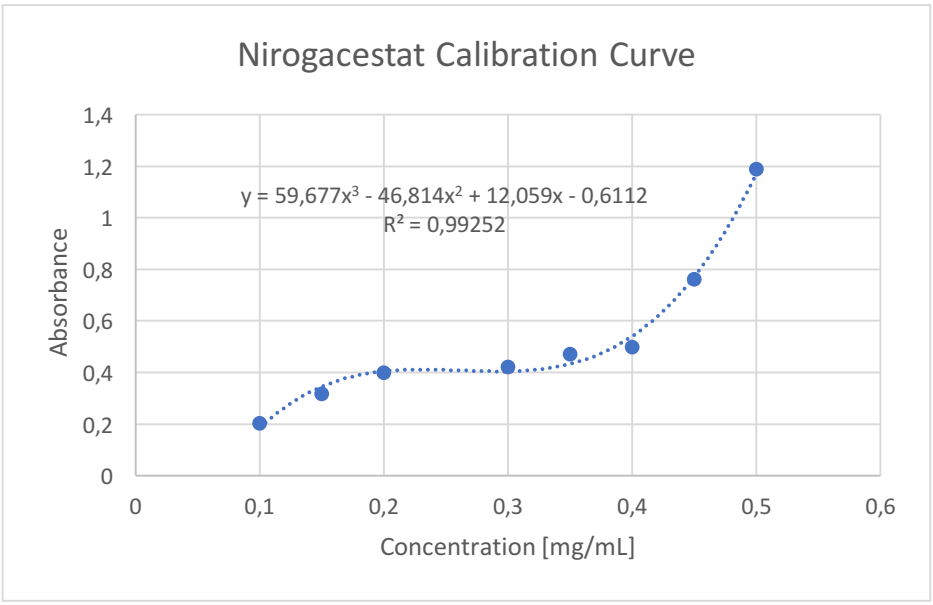

Fig. 3.11. Nirogacestat calibration curve.

To do this, an initial stock solution consisting of nirogacestat in acetonitrile (1 mg/mL) was made. Eight standard samples across a range of concentration near that one expected were prepared, implementing the dilution, from 0.10 mg/mL to 0.45 mg/mL, using acetonitrile. The spectra, obtained subjecting the samples to a 248 nm wavelength light, showed peaks, even if unstable, around 248 nm. A third-degree polynomial was used to fit the experimental points and the value of the coefficient of determination, $R^2 = 0.99252$, means that data are very closed to the fitted regression line.

3.3 Ink Characterization

3.3.1 Ink Constituents

To reduce the number of experiments needed to pick out the ink formulation we took account of studies previously done regarding the influence of the fluid properties on the printability, since different fluid compositions present distinct optimal printing conditions, otherwise the procedure would be extremely time consuming. D. Jang et. Al. (2009), based on numerical analysis performed by computational fluid dynamics models, have experimentally proved that the printable range is defined for values of Z between 4 and 14.

As first attempt, different combinations of MQ and PG were chosen. In contrast with the results obtained in previous studies[42], in which as co-solvent formulation was chosen equal parts of PG and MQ (50:50), adapting the same printing settings, only a few nozzles were working.

Tab. 3.2. Ink formulations. Values regarding different PG:MQ formulations are taken from 'Inkjet Printing of Drug-Loaded Mesoporous Silica Nanoparticles – A Platform for Drug Development'. Density of MQ:PG:IPA formulations is measured at 32°C. High IPA volatility could lead to discrepancies between theoretical and experimental density values.

PEI MSN concentration [mg/ml]	MQ	PG	IPA	Viscosity [Pa s, 25°C]	Density [kg/l]	Surface tension [mN/m]	Z value
	50	50		0.0052	1.048	44.82	9.32
	60	40		0.0036	1.022	44.10	13.18
	70	30		0.0026	1.024	49.61	19.38
	20	20	60	0.0039	0.8040	27.29	2.68
	20	30	50	0.0048	0.8785	24.01	6.76
	20	10	70	0.0032	0.8027	27.03	10.29
	30	20	50	0.0038	0.8652	28.85	9.29
0.5	20	20	60	0.0039	0.8562	23.86	8.19
1	20	20	60	0.0040	0.8445	27.53	8.52

Viscosity and surface tension modifications were done. To reduce viscosity, two solutions in 40:60 and 30:70 (v/v) ratios of PG:MQ were prepared to avoid any clogging of the nozzles, but this could irremediably raise the Z-value, achieving undesirable results (Table 3.2). In fact, the increasing volume of MQ led to lower viscosity values, but at the same time higher surface tension values.
For that reason, after having ascertained the drug insolubility in isopropanol, since the MQ:IPA 50:50 (v/v) already was closed to the border of jettable fluids in terms of surface tension, we decided to introduce IPA to the ink base. The reduction of surface tension was of crucial impact for the jettability of the ink. A formulation made by MQ, PG and IPA was chosen. MQ:PG:IPA in 20:10:70 (v/v) and 30:20:50 (v/v) were excluded because of the too much high Z value, compared to the suggested ones by literature. Two formulations of MQ:PG:IPA 20:20:60 (v/v) and 20:30:50 (v/v) were tried, but we preferred the first one since the second one involved nozzles clogging.
Also the possibility to use ethanol was considered, but the proved dissolution of drug in ethanol[46] could definitely cause an undesired drug leaching during the printing process.

3.3.2 Ink Characterization results

The suspension was obtained through a chronological dispersion of silica mesoporous nanoparticles firstly in water and then in PG and IPA, that were simultaneously added under sonication to the MQ and MSNs dispersion, as suggested from researches previously done.[42]
The tested suspensions consisted of four several concentration samples (0.1, 0.5, 1 and 5 mg/mL) of spherical MSNs per each stock: one of them FITC labeled and the other PEI surface functionalized. Dynamic light scattering measurements (Table 3.3) were done to evaluate the dispersity of nanoparticles inside the ink and to confirm that the particles size is lower than the value (2 μm) advised by the manufacturer.

Tab. 3.3. DLS of MSNs in MQ:PG:IPA 20:20:60 (v/v) varying concentration.

Sample	Concentration [mg/mL]	Particle Size [nm]	PDI
PEI-FITC	0.1	554.87 ± 70.7	0.604 ± 0.42
	0.5	563.67 ± 36.1	0.035 ± 0.03
	1	586.23 ± 18.5	0.048 ± 0.03
	5	658.96 ± 96.8	0.073 ± 0.06
FITC	0.1	664.37 ± 364.3	0.683 ± 0.48
	0.5	640.07 ± 6.25	0.057 ± 0.03
	1	626.66 ± 10.7	0.122 ± 0.09
	5	632.23 ± 67.2	0.219 ± 0.20

According to literature the volume distribution value[44] should preferably be fifty times lower than the nozzle diameter (50µm) to avoid any risk.[43]
Fig. 3.2 (section 3.1.1) shows uniform size distribution of 1% APTES-FITC MSNs in ink formulation (1 mg/mL) and an average size value in line with what just said.

Both loaded and unloaded ink formulations, as can be seen from Figure 3.12, showed a constant value of viscosity, meaning that the linear proportionality between shear rate and shear stress of the dispersing mix is still valid, even if the presence of nanoparticles caused a weak increase of the slope.

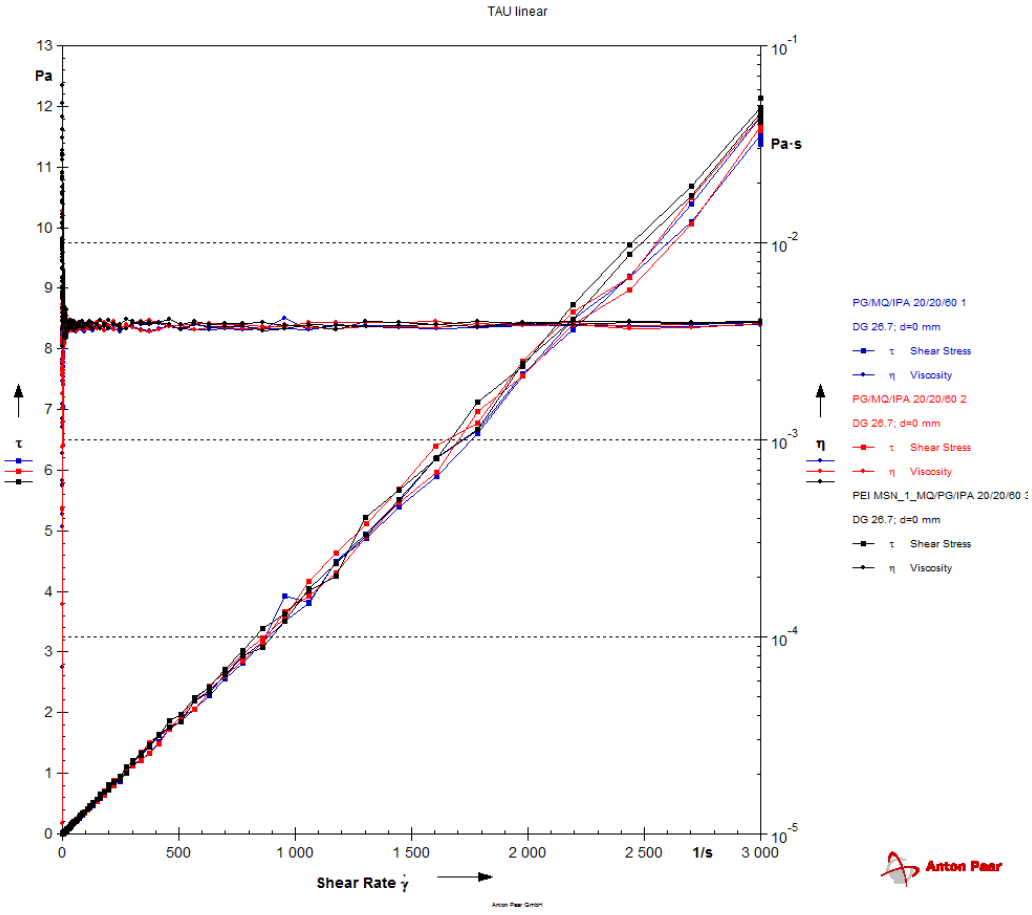

(a)

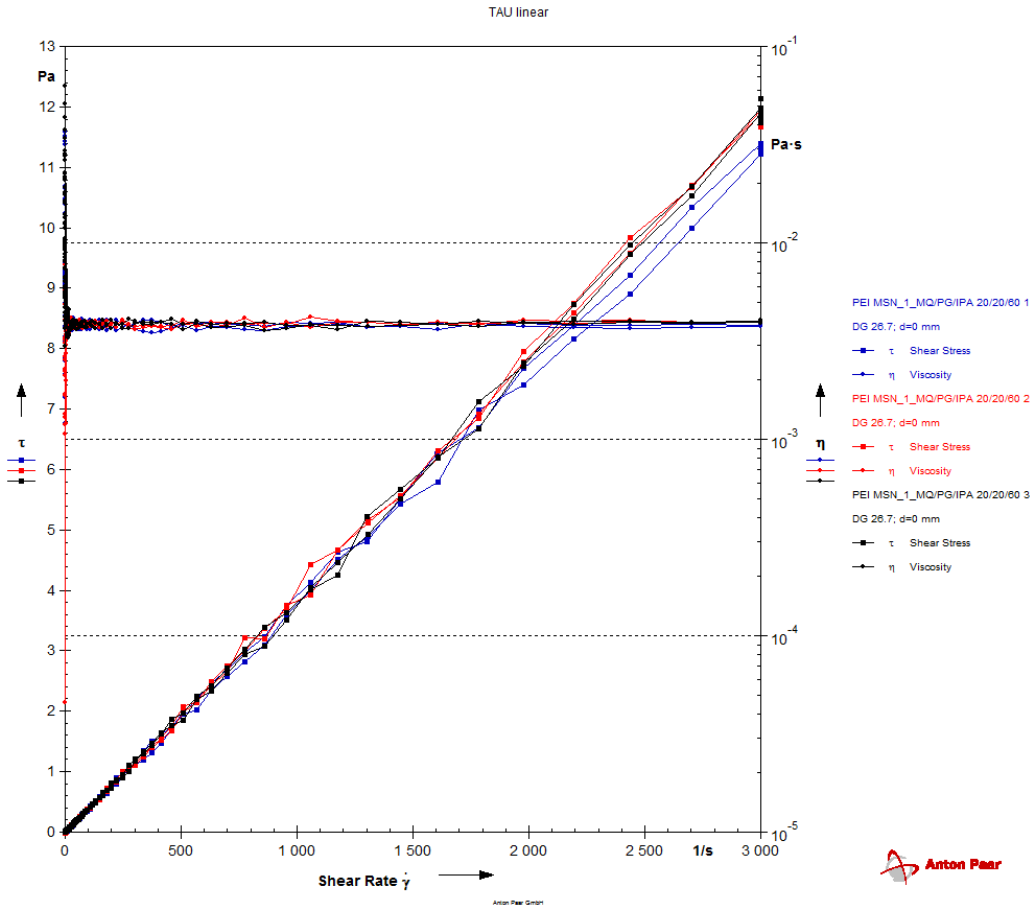

(b)

Fig. 3.12. (a) Viscosity measurement of ink formulation. (b) Viscosity measurement of 1% APTES-FITC PEI functionalized in MQ:PG:IPA 20:20:60 (v/v) (1 mg/mL).

3.4 Drug Leaching

At first, drug release in IPA was monitored, since the known hydrophobicity of the drug ensures the lack of its dissolution in propylene glycol and distilled water. A stock solution was made consisting of drug 10 wt% (0.5 mg) loaded in nanoparticles (5.3 mg) collected in 2 mL of IPA (concentration 2.5 mg/mL).

After 3 hours a 0.29 absorbance of the surfactant was observed through UV-Vis at 248 nm, corresponding to 0.128 mg/mL drug leaching. Instead, after 5 hours the amount of drug released was lower (0.017 absorbance corresponding to 0.069 mg/mL), meaning that the remaining content is completely kept inside the pores. The same procedure was followed with the ink formulation. 0.25 mg (5 wt%) of nirogacestat was loaded in 5 mg of 1% APTES-FITC MSNs PEI functionalized, that were dispersed in 5 mL of MQ:PG:IPA 20:20:60 (%vol), in order to mimic the same printing solution (1 mg/mL). The leaching test was conducted after 3 and 5 hours.

After 10 minutes 10000 rpm centrifugation, the drug content was measured from the supernatant. After three hours, an average absorbance of 0.154 (Figure 3.13(a)) meant a release of drug in the ink formulation equal to 0.094 mg/mL. Instead, after five hours, an absorbance of 0.018 (Figure 3.13 (b)) fits a concentration almost naught.

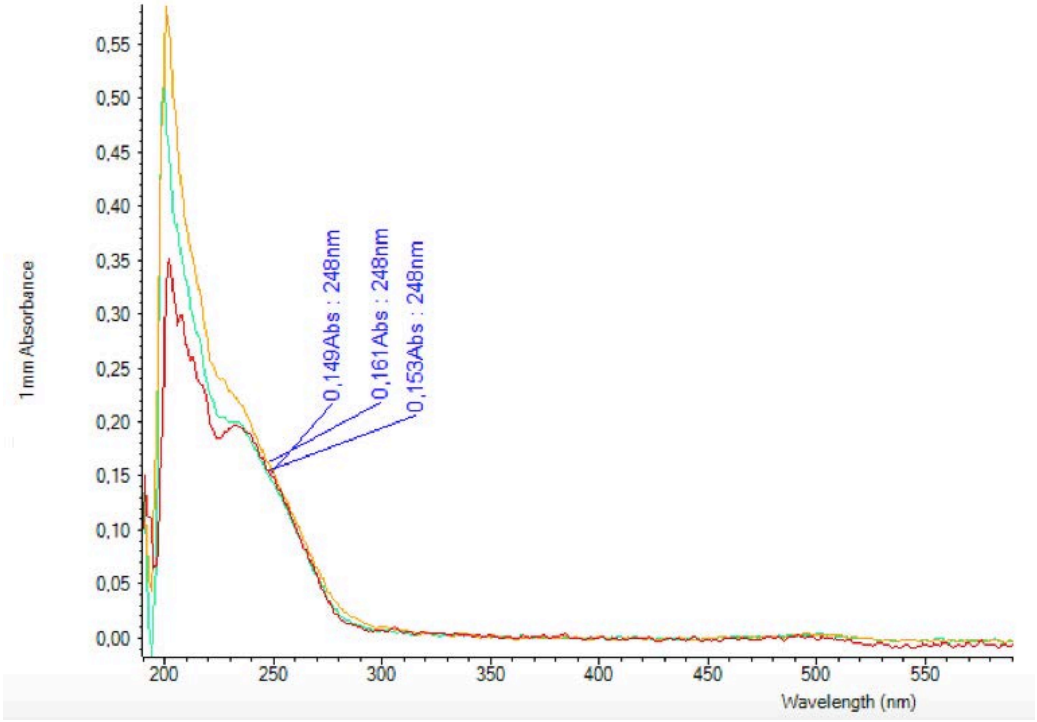

(a)

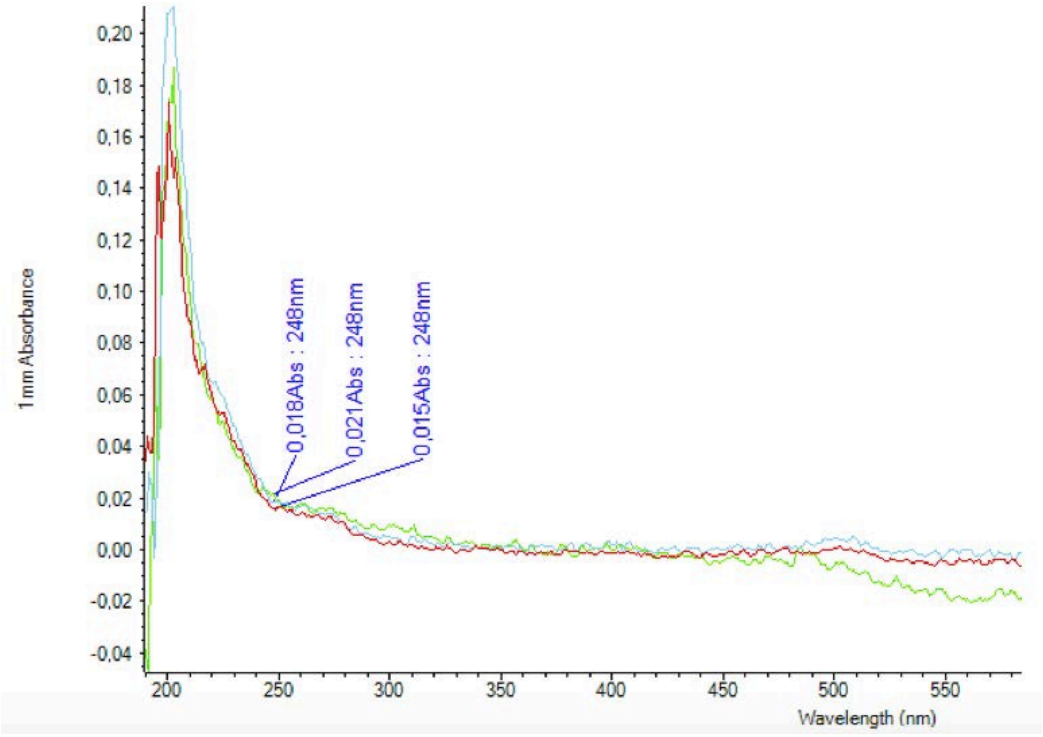

(b)

Fig. 3.13. Uv-Vis analysis for drug leaching (a) after 3 hours rotation. (b) After 5 hours rotation.

3.5 Printing Process and droplet analysis

3.5.1 Optimization of Printing Settings

The optimization of the setting was initially done by adjusting the ink pressure considering that if it's too low air bubbles might enter the container causing nozzles clogging, while a too high value could give rise to leaking problems. The ink pressure was set to -19.5 mbar.
To print the ink 33 nozzles were used, because they showed more precise droplets formation.
By activating the advanced drop analysis and defining an increment time step of 50 µs from an initial value of 0 µs till 500 µs of the moment the photo is taken after the trigger, we have monitored the behavior of the drop formation over time.
As can be noticed from the Figure 3.14 (a) the desired droplet shape is obtained, even if it's characterized by a jumping unstable trend, probably caused by the interference with the surrounding droplets. Anyway, a just one nozzle printing would ensure a major stability. While, in Figure 3.14 (b), the settings need to be optimized to avoid satellites formation.

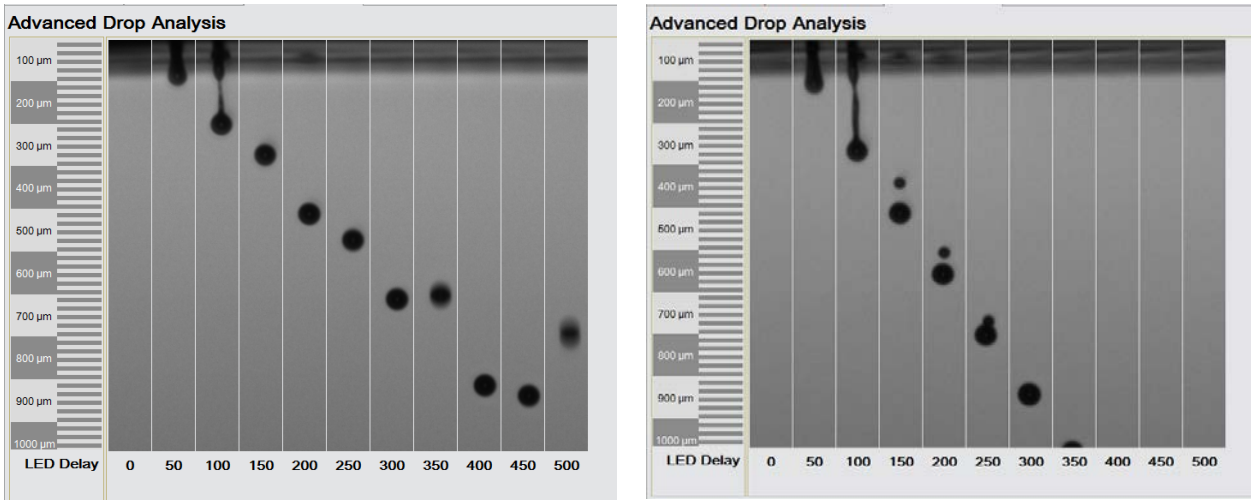

(a) (b)

Fig. 3.14. Advanced Drop Analysis of unloaded 1% APTES-FITC MSNs in MQ:PG:IPA 20:20:60 (v/v).

Trials carried out before[42] pointed out a weak influence of nanoparticles, into the ink formulation, regarding the printing settings. Three formulations of unloaded PEI functionalized MSNs dispersed in the ink (0.1, 0.5, 1 mg/mL) were printed, considering that 5 mg/mL concentration showed a low printability, maybe due to sedimentation of them inside the container that caused nozzles clogging. The printing was performed by maintaining an ink pressure value equal to -19.5 mbar and voltage to 99 and 85 V, but the pulse shapes of odd and even nozzles were respectively set to 8-5, 15-15.5, 8-5. Just to prove the printability of dispersed MSNs in the ink formulation, a resolution of 500 DPI was initially set for all the three dispersions.

After that, other trials increasing the number from 100 to 500 DPI were performed. We have printed just one layer on the substrate, even if more than one help to increase the concentration of nanoparticles. After having identified the 1 mg/mL as the most concentrated printable solution, we have proceeded with the printing of unloaded and loaded nanoparticles. Unloaded nanoparticles were printed using eleven nozzles (number 1, 2, 4, 5, 9-15), that camera ensured to guarantee the better drop shapes. While drug loaded nanoparticles were deposited on the substrate through 12 nozzles (1, 2, 5-14). Moreover, the printing setting values for loaded nanoparticles were adjusted to 91, 85 V and 8-5, 15-14, 8-5 regarding the pulse shape.
Moving of 2.4 cm, thanks to 'teach and go to' mode, the position of the printer head after having printed on 4 circles, was possible to print with 5 different resolutions on the same substrate. The average droplet volume was 38.8 pl and 40.2 pl respectively for unloaded and loaded MSNs.

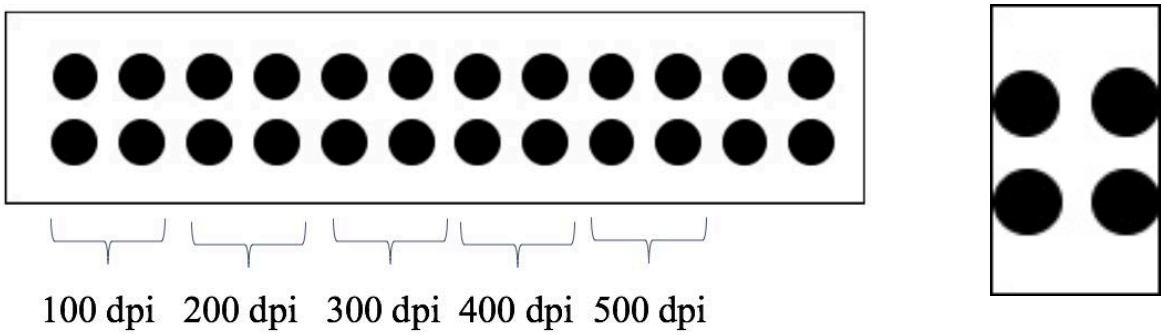

Fig. 3.15. (a) Printing Process. (b) Pattern width=2.4 cm, space between each circle = 0.4 cm, distance from the top and the bottom = 0.75 cm.

For 100 DPI, the printing of unloaded MSNs was also performed only with nozzle number 13 (droplet volume=37.1 pl), that accommodated the best drop shape.
After printing, the unloaded and loaded printed substrates were stored inside a plastic transparent case (Genomic Solutions Cons 100) for 5 and 2 days, respectively, before the microscopic analysis, wrapped in aluminum foil and kept at room temperature (22 °C) in dark conditions, to avoid any interactions between FITC and the light.

3.5.2 Dose Quantification

With 1000 Hz firing frequency printing, based on the area of the paper circles (8 mm diameter) and the resolution, the number of droplets can be defined. Knowing the average ejected droplet volume of 1mg/mL suspension, it's possible to determine firstly the volume of PEI MSNs per single circle and secondly also the mass, knowing the concentration. Additionally, since 5 wt% drug loading was carried out, dose quantification can be calculated:

$$volume\ of\ \text{MSN PEI printed} = \text{average drop volume} \times \text{resolution} \times \text{area}$$

Tab. 3.4. Dose Quantification.

Resolution [DPI]	**100**	**200**	**300**	**400**	**500**
Volume of unloaded PEI MSNs [x 10^{-6} mLxcm]	0.7678	1.535	2.303	3.071	3.838
Mass of unloaded PEI MSNs [x 10^{-6} mgxcm]	0.7678	1.535	2.303	3.071	3.838
Volume of loaded PEI MSNs [x 10^{-6} mLxcm]	0.8002	1.6004	2.4006	3.2601	4.001
Mass of loaded PEI MSNs [x 10^{-6} mgxcm]	0.8002	1.6004	2.4006	3.2601	4.001
Nirogacestat [x 10^{-6} mgxcm]	0.04	0.08	0.12	0.16	0.20

3.5.3 Substrate Interactions

The substrate is composed by 24 cardboard wells derived from a LATEX coating on a cardboard rectangular film. We have noticed a similarity of contact angles between the ink formulation and the nanoparticles loaded ones. In all the cases, low contact angles (20°, 24.35°, 25.35° respectively for ink, 0.5 mg/mL and 1 mg/mL) were measured on the circles, after 6 seconds.

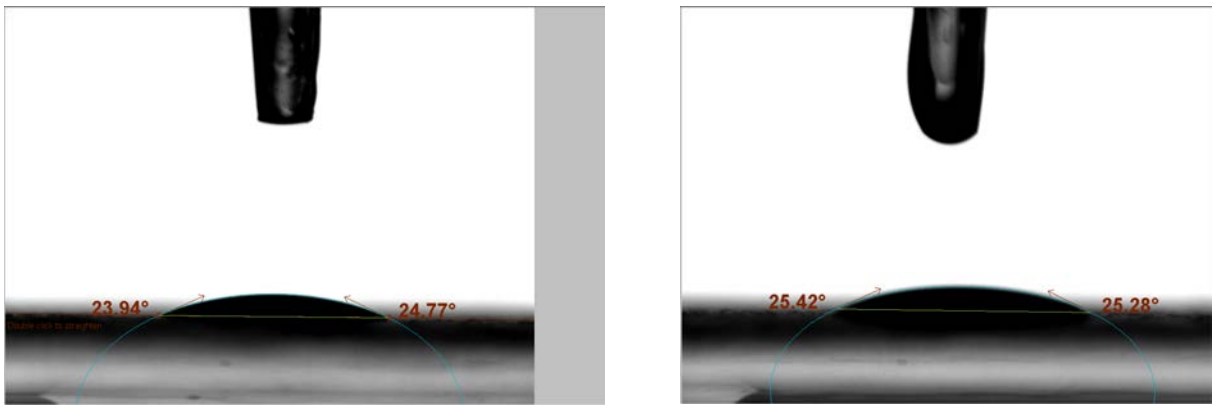

(a) (b)

Fig. 3.16. (a) 0.5 mg/mL PEI 1 %APTES-FITC MSNs contact angle on cardboard. (b) 1 mg/mL PEI 1% APTES-FITC MSNs contact angle on cardboard.

After the same amount of time, 53°, 61° and 63° were showed on the transparency polyester film. The proximity of latex doesn't affect the measure of contact angle on the cardboard, if the droplet is small enough and placed on the cardboard. Alternatively, latex will limit the drop from spreading.

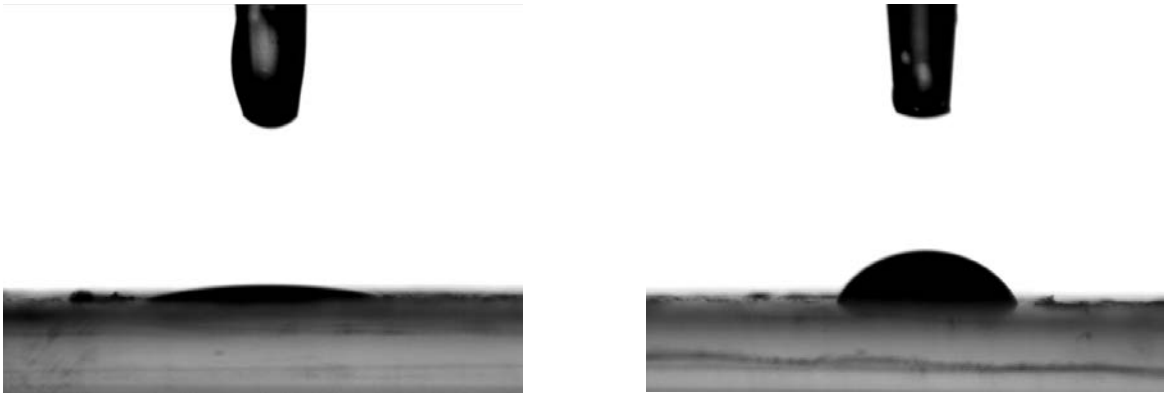

(a) (b)

Fig. 3.17. (a) Contact angle of 1% APTES-FITC MSNs in ink formulation (1mg/mL) on cardboard (25.35°). (b) On latex (63°). Measurements performed after 6 seconds.

3.6 Printed Samples Characterization

3.6.1 Fluorescence Confocal Microscope

Confocal microscopy has shown that MSNs appear not homogenously spread on the droplet, giving rise to a deposit along the perimeter of it as well as formation of clusters inside, for both drug loaded and unloaded 1% APTES FITC MSNs PEI functionalized (Figure 3.18).

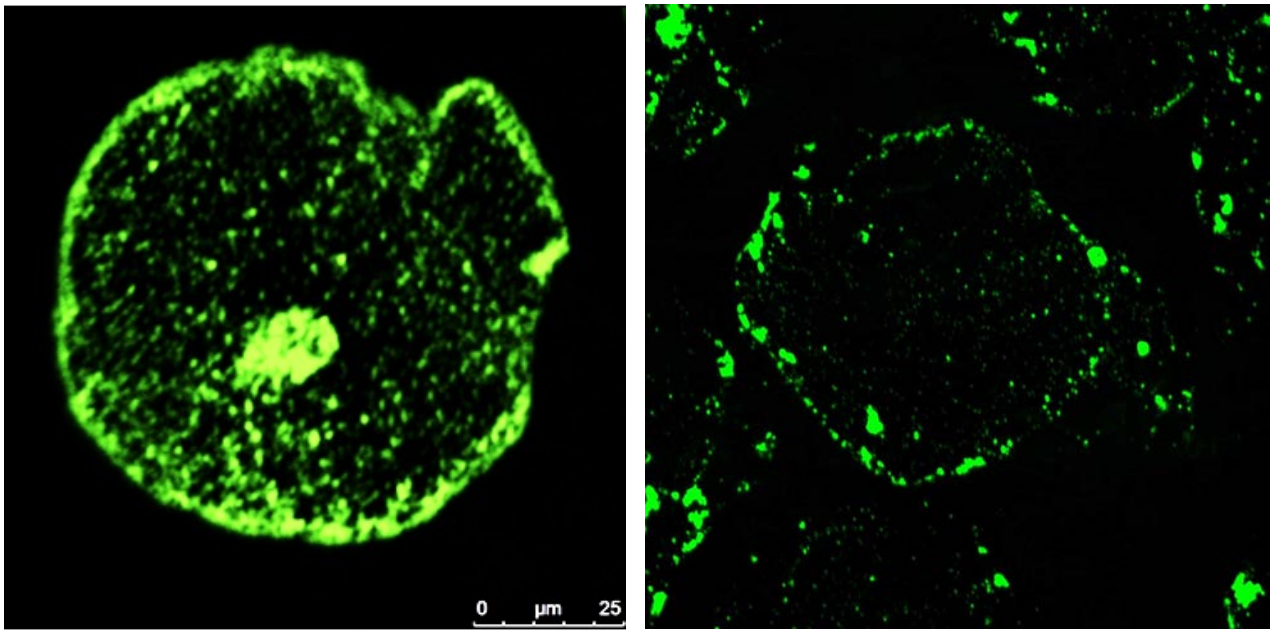

(a) (b)

Fig. 3.18. Confocal Laser Scanning Microscope (CLSM) images of (a) 1 mg/mL unloaded 1% APTES-FITC MSNs PEI functionalized in ink formulation (100 DPI). (b) 1 mg/mL loaded 1% APTES-FITC MSNs PEI functionalized in ink formulation (300 DPI).

The ‘coffee ring’ pattern, due to interactions between ink and substrate and drying process, negatively affects nanoparticles uniform distribution, that the ink jet printing should guarantee. The difference between the evaporation rates across the droplet, causes a liquid flow towards the edge of it. The evaporation induces a not enough Marangoni flow inside the droplet which could redistribute the liquid, as originally printed. Only the adding of surfactants could disrupt the initial towards sides flow, avoiding detrimental of the pattern, but this would affect the printability of the ink.
For resolutions till 300 DPI, droplets present not a massive size difference (80 μm) and an approximately spherical shape, while for 400 and 500 DPI they are merged (Figure 3.19).

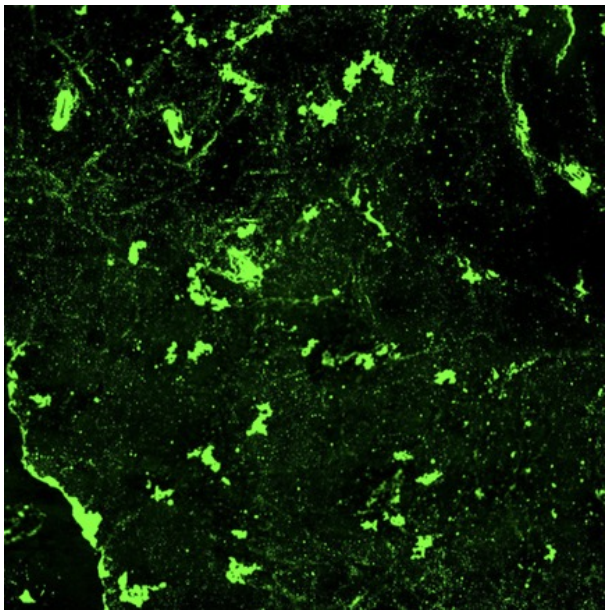

Fig. 3.19. Confocal Laser Scanning Microscope (CLSM) image of 1 mg/mL loaded 1% APTES-FITC PEI functionalized in ink formulation (500 DPI).

4. DISCUSSION

4.1 MSNs Characterization

Based on all the assumptions, according to literature (section 2.1 and 2.2), MSNs were characterized by different techniques (chapter 3).

The polydispersity index, represented by a dimensionless value between 0 and 1, compares the distribution width with the distribution mean.[23] A polydispersity index of 0.048 for unloaded 1% APTES-FITC MSNs dispersed in the ink formulation (1 mg/mL) was calculated, indicating a monodisperse suspension, as can be noticed from Figure 3.2.

To measure the precise size of nanoparticles, Trasmission Electron Microscopy analysis were performed. Unfunctionalized 1% APTES-FITC MSNs diameter was about 180 nm with 1% margin of error, according with the value suggested.
Performing characterization of 1% APTES-FITC MSNs after PEI functionalization, J. M. Rosenholm et al. (2007) have shown that NPs diameter remains virtually the same, although the BET specific surface area and the total pores volume decrease due to the increase of mass of the material. Furthermore, their studies proved that the PEI functionalization is indeed preferentially located on the outer surface of the particles if the functionalization step is carried out before surfactant extraction; instead, as our case, if it's done after the surfactant removal, also the internal mesoporous network is superficial modified. PEI grafting procedure doesn't modify MSNs shape and seems to avoid pores radial distribution modifications, as can be noticed in Figure 4.1.

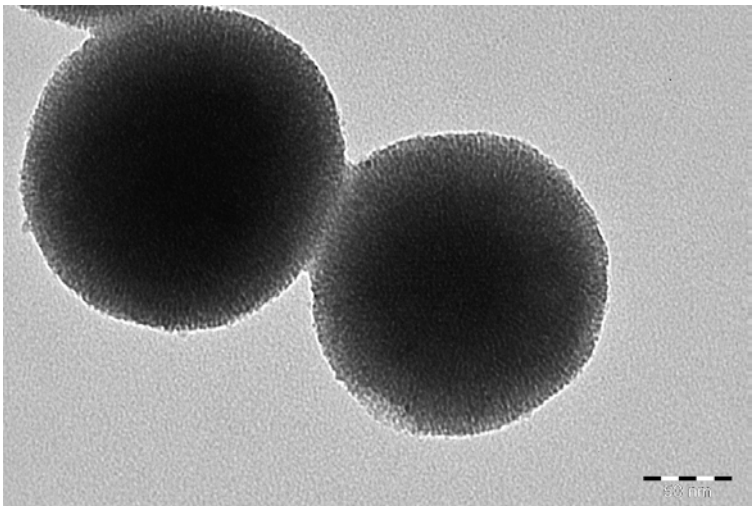

Fig. 4.1 TEM image of PEI functionalized 1% APTES-FITC MSNs.

In order to quantify the exact amount of PEI grafted on the surface, TGA analysis is requested. However, Zeta Potential measurements can be performed after grafting as process control.
Zeta Potential should be shifted toward higher values, compared to those ones obtained in 3.1.1. section, due to the presence of positively charged $-NH_3^+$ groups on the outer particle surface[34]; so, to assess if the grafting has been successfully performed or not, its average value before and after grafting was evaluated:

Tab. 4.1. Comparison of physicochemical properties before and after grafting of 1% APTES-FITC MSNs.

Before Grafting		**After Grafting**
Z – Potential: - 8.3 mV	→	Z – Potential: + 27.87 mV
Conductivity: + 0.552 mS/cm	→	Conductivity: + 0.603 mS/cm
Size: 401 nm	→	Size: 338.3 nm
Concentration: 24 mg/ml	→	Concentration: 26.4 mg/ml

The average of three Zeta Potential measurements showed an increase from -8.3 mV to +27.87 mV, proving PEI grafting efficiency. Furthermore, even if the conductivity remained almost the same, we could notice an increase of particles concentrations and especially a decrease of particles size.
Regarding PEI unfunctionalized MSNs, as rule of thumb, it's assumed that the general dividing line between a stable and unstable suspension is at +30 mV or -30 mV.[26] However, the presence of surfactant affects the value, that would be weakly negative compared to the expected ones (-10, -20 mV).

Tab. 4.2. Z – Potential and Conductivity values of all the batches.

Type of batch	**Zeta Potential [mV]**	**Conductivity [mS/cm]**
Bare MSNs	-19	+ 0.5
1% APTES-FITC MSNs	-7.3	+ 0.551
5% APTES-FITC MSNs	-5.3	+ 0.572
10 % APTES-FITC MSNs	-3	+ 0.518
1% APTES-FITC MSNs (400 mL)	-8.3	+ 0.552

The first surface charge evaluation was done for the first batch synthesized, so for bare nanoparticles, and the value obtained, as we can see from Table 4.2, agreed with the expectation. So, from the surface charge point of view, the synthesis was considered successful. Conductivity, that's an indication of the charge strong, shouldn't be below + 0.4-0.5 mS/cm. If a value closed to 0 was obtained, it meant that the charge was just due to the solvent, not to the particles.

Experiments have shown the percentage increase of dye causes a decrease of negative surface charge and the reproducibility of 1% APTES-FITC, since, regarding charge and conductivity values, there was no relevant difference between the two batches.
The value of Zeta Potential was sufficiently negative to say that the suspensions were stable (Table 4.2) and the volume distribution value (Table 4.3), as said in 3.3.2 section, was fifty times lower than the nozzles diameter.

Tab. 4.3. Diameter and PdI of all the batches.

Type of batch	Z-average d [nm]	PdI
2MSP bare	380	0.1
2MSP 1% APTES - FITC	637.6±54.84	0.271
2MSP 5% APTES - FITC	310±3.23	0.099
2MSP 10% APTES - FITC	801.8±59.7	0.198
2MSP 1% APTES – FITC (400 mL)	401	0.151

The reason why particles aren't perfectly spherical (Figure 3.7) isn't due to collisions with other particles, since they repeal each other, but to the sonication and vortexing procedure. Also the drying time could cause the same effect.
The arches than can be seen in Figure 3.7 are due to the presence of liquid. As earlier mentioned in 2.3 section, the choice of the extraction technique could affect the final result, because surfactant residues can be still stacked on the MSNs surface. Washing it completely out is important to avoid interactions with the drug.
400 mL 1% APTES-FITC MSNs PEI functionalized offered all the structural properties we were looking for.

4.2 Ink base Properties

The selection of ink constituents was performed based on the calculated Z value (Table 3.2) and its limit suggested by literature, as earlier explained in 3.3.1 section, bearing in mind the interactions between nirogacestat and chosen chemicals, to avoid any drug leaching before the printing.
Figure 3.13 (a) and (b) confirmed that the nirogacestat repulsion towards MQ and PG, due to the hydrophobicity of the drug, disadvantages the dissolution of drug inside the ink. Drug release from MSNs, that were kept rotating for 3 and 5 hours, was negligible in the first case, while almost naught in the second ones.

Physicochemical properties of MSNs both unfunctionalized and PEI functionalized, dispersed in the ink base, were analyzed for 4 several concentrations.
Reassured that the hydrodynamic diameters that DLS provides are overstated compared to those ones got from other more detailed techniques, such as TEM, this analysis (Table 3.3) confirmed that both

MSNs dispersions, in all investigated concentrations, satisfy the limiting condition imposed by D. Kuscer et al. (2012). Large polidispersity index values, detected for both 0.1 mg/mL concentration stocks, showed an aggregated colloidal solution formation, that means inaccuracy of the obtained diameter data. The real particles size, in these samples, should be smaller, in any case not concerning clogging issues. These data ensured unloaded nanoparticles dispersity in the selected co-solvent mixture. The drug loading won't affect the DLS results.[44]

MSNs addition in the ink formulation, as noticed by J. Park et al. (2006), didn't dramatically affect the viscosity, much less modifying the original Newtonian behavior of the fluid (Figure 3.12).

In line with the studies of J. Hyväluoma et al. (2003), viscosity (Table 3.2) is subjected to increase with particles concentration, while the surface tension values remain the same.
However, all these measures on which Z value is derived, are related to a temperature higher than the operative ones. Hence, although they represent a starting point for all the considerations done about the ink printability (section 3.3.1), they still remain indicative. A more accurate prediction of the ink jetting behavior could be made only if the liquid characterization would be performed at the same printing temperature (23°C). Besides, we have assumed that the ink is subjected to a maximum shear rate that rheometer can reach (3000 1/s), characterizing it when extremely solicited, even if during the printing the shear rate reaches value around 10000 1/s.[50]

The dynamic measurements of contact angles (section 3.5.3) demonstrated a dependency on the MSNs amount, since a few degrees units increment was observed increasing MSNs concentration.
The pronounced difference between the contact angles of liquid on cardboard, that it's used in the development of delivery medicament since its inactivity with ionic species, and latex film shall ensure a net posting between the circles, where the drug uptaken by cancer cells is assessed, and the rest of the substrate where cells are not stored.

4.3 Drug Leaching

Data obtained in 3.4 section concerning the content of drug released in IPA and in the ink base after 3 and 5 hours rotation can be influenced by the presence of surfactant.[45] High Perfomance Liquid Chromotography (HPLC) should be preferred because it allows to separate and quantify each components in the mixture. It permits to obtain a more reliable indication of the drug concentration inside the ink formulation, since the drug amount released by MSNs seems to be not negligible.

4.4 Printed Samples

100, 200 and 300 DPI didn't pass on the printing quality since almost spherical and well defined droplets has been obtained (Figure 4.2); however, the increase of resolution and so of the number of dots per inch, decreased the distance between each single droplet, leading them to merge (Figure 3.18).
Secondly, the high volatility of the ink, which is mostly composed by isopropanol (IPA), delays the adsorption on the paper, making competitive the adsorption and merging rates. If the second one prevails over the first one, the result is that one we can see in Figure 3.19.

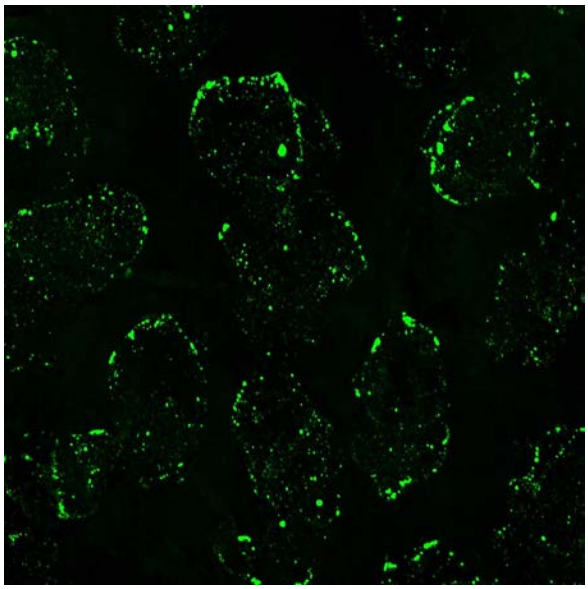

Fig. 4.2. Confocal Laser Scanning Microscope (CLSM) images of (a) 1 mg/mL unloaded 1% APTES-FITC MSNs PEI functionalized in ink formulation (200 DPI).

Not homogeneous distribution of MSNs on droplets (Figure 3.18) may be explained by sedimentation, that has taken place in the time between container filling and printing, or on the low contact angles (23°) between ink and cardboard.

For similar PEI functionalized MSNs has been reported[54] how the nanoparticles concentration influences the signal. Even if it is well known the self quenching effect, due to fluorophores vicinity[55], which makes the tracking unfeasible, on the contrary an higher concentration of FITC labeled MSNs gives rise to a greater fluorescence intensity. In fact, the distribution of fluorophores inside the porous network provides the advantage to print them closely, without affecting the confocal detection.
From the fluorescence intensity signal, produced by unloaded and loaded nanoparticles printed with different resolutions on the substrate, could be interesting to find out a relation between the fluorescence and the MSNs dose. However, since Fiji Imagej software intensity measurements depend on the brightness and contrast values, these data are not reliable.

5. CONCLUSION

Printing in pharmaceutical field is a promising technology that offers individual treatment solutions; so in the future it's expected an even closer cooperation between researchers and industry to improve this new manufacturing approach that's able to provide flexible dose adjustments, based on the patient. This great opportunity, that hopefully could lead to a 'print at home' approach, needs to be carefully evaluated and optimized, since many aspects, such as shape, materials, surface area, influence the final properties of the dosage form as well as its safety[59] and albeit a small variation of parameters could have consequences contrary to those desired.

In this project, 1% APTES-FITC MSNs were firstly manufactured and functionalized and then dispersed with different concentrations inside the inkbase MQ:PG:IPA 20:20:60 (v/v), that was chosen base on the Z-values obtained. Both loaded and unloaded MSNs (1 mg/mL) were printed on the substrate.

Printing settings were optimized for a new ink formulation; however, even if the adding of isopropanol ensures printability, the drug leaching quantified using UV – Vis is not negligible. Only the use of the High Performance Liquid Chromatography can determine if data provided by the above mentioned technique are reliable or not, considering that in studies previously done[45] the presence of surfactant changes the adsorption values, affecting the predicted drug release.

Characterization methods showed that both synthesis and surface functionalization processes have been performed successfully.

By developing and optimizing the ink formulation, the aim to achieve a high precision of printing, theoretically ensured by a drop on demand ink jet printing, has been proved since no fluorescence traces were disposed between the circles for resolutions below 300 DPI. However, this technique needs to be upgraded since all the after printing analysis have shown reproducibility problems, regarding the drop dimensions. Even for the dose quantification, we have considered the average volume of the droplets, that slightly changes impacting the paper. So, even though the drug amount printed depends on the known mass of nanoparticles ejected, their volume distribution doesn't cause drug uniformity on the cardboard circles, affecting the quantity up taken by the cells in a specific region. For this reason, a further improvement of size control should be implemented and a first solution to prevent particles aggregation, that takes place right before the ink ejection, could be a stirrer equipped container.

Figure 4.2 shows that the droplets are not spatially placed even if the chosen inkbase, based on table 3.2, should guarantee better performances than those ones obtained with MQ:PG formulations.[45] For that reason, different setting parameters would have been needed to get a spatial drop deposition.

6. SYMBOLS AND ABBREVIATIONS

2D	Two Dimensional
3D	Three Dimensional
API	Active Pharmaceutical Ingredient
APTES	(3-Aminopropyl)triethoxysilane
BET	Brunauer-Emmett-Teller (BET) Surface Area Analysis
BJH	Barrett-Joyner-Halenda (BJH) Pore Size Distribution Calculator
CLSM	Confocal Laser Scanning Microscope
CTAB	Cetyltrimethylammonium Bromide
DLS	Dynamic Light Scattering
DoD	Drop on Demand
DPI	Dots Per Inch
EPR	Enhanced Permeability and Retention Effect
FITC	Fluorescein Isothiocyanate
GMP	Good Manufacturing Practice
HEPES	4-(2-hydroxyethyl)-1-piperazineethanesulfonic acid
HPLC	High Performance Liquid Chromatography
HS	Helmotz-Smoluchowski
IPA	Isopropyl Alcohol
K_B	Boltzmann Constant
MDR	Multidrug Resistance
MSNs	Mesoporous Silica Nanoparticles
MSP	Mesoporous Silica Particles
NBCDs	Non Biological Complex Drugs
NC	Nanocarrier
NPs	Nanoparticles
η	Medium Viscosity
Oh	Onhesorge Number
PdI	Polidispersity Index
PEG	Polyethylene Glycol
PEI	Polyethyleneimine
PG	Propylene Glycol

PIJ	Piezoelectric Inkjet
PZC	Point of Zero Charge
QF	Quality Factor
R_H	Hydrodynamic Radius
Re	Reynolds Number
RES	Reticuloendothelial System
SDA	Structure-Directing Agent
T	Absolute Temperature
TEM	Transmission Electron Microscopy
TGA	Thermogravimetric Analysis
TIK	Thermal Inkjet
UV-vis	Ultraviolet Visible Spectroscopy
We	Weber Number
ζ- Potential	Zeta Potential

7. REFERENCES

[1] BERGMAN, L., 2014. Influence of surface functionalization on the behavior of silica nanoparticles in biological systems, Laboratory of Physical Chemistry, Åbo Akademi (2014).

[2] KARAMAN, D. S., 2016, Physiochemical characteristic of silica nanoparticles tailore for nanomedicine, Laboratory of Physical Chemistry, Åbo Akademi (2016).

[3] BRINKER, C.J., 1988. Hydrolysis and condensation of silicates: effects on structure. *Journal of Non-Crystalline Solids,* **100**(1-3), pp. 31-50.

[4] STÖBER, W., FINK, A. and BOHN, E., 1968. Controlled growth of monodisperse silica spheres in the micron size range. *Journal of colloid and interface science,* **26**(1), pp. 62-69.

[5] JANA, S.K., MOCHIZUKI, A. and NAMBA, S., 2004. Progress in pore-size control of mesoporous MCM-41 molecular sieve using surfactant having different alkyl chain lengths and various organic auxiliary chemicals. *Catalysis surveys from Asia,* **8**(1), pp. 1-13.

[6] LIM, J., HA, S. and LEE, J., 2012. Precise size-control of silica nanoparticles via alkoxy exchange equilibrium of Tetraethyl Orthosilicate (TEOS) in the mixed alcohol solution. *Bulletin of the Korean Chemical Society,* **33**(3), pp. 1067-1070.

[7] LEE, K., LOOK, J., HARRIS, M.T. and MCCORMICK, A.V., 1997. Assessing extreme models of the Stöber synthesis using transients under a range of initial composition. *Journal of colloid and interface science,* **194**(1), pp. 78-88.

[8] Biodiesel.org. 2015. *Frequently Asked Questions About the Safe Handling & Use of Methanol*. [ONLINE] Available at: http://biodiesel.org/docs/ffs-methanol/faq-about-the-safe-handling-and-use-of-methanol.odf?sfvrsn=6. [Accessed 29 June 2018].

[9] MALAY, O., YILGOR, I. and MENCELOGLU, Y.Z., 2013. Effects of solvent on TEOS hydrolysis kinetics and silica particle size under basic conditions. *Journal of Sol-Gel Science and Technology,* **67**(2), pp. 351-361.

[10] INNOCENZI, P., 2016, The Sol to Gel Transition, chapter 2: From the Precursor to a Sol, Springer Briefs in Materials.

[11] CHIANG, Y., LIAN, H., LEO, S., WANG, S., YAMAUCHI, Y. and WU, K.C., 2011. Controlling particle size and structural properties of mesoporous silica nanoparticles using the Taguchi method. *The Journal of Physical Chemistry C,* **115**(27), pp. 13158-13165.

[12] MALEKI, A., KETTIGER, H., SCHOUBBEN, A., ROSENHOLM, J.M., AMBROGI, V. and HAMIDI, M., 2017. Mesoporous silica materials: From physico-chemical properties to enhanced dissolution of poorly water-soluble drugs. *Journal of Controlled Release,* **262**, pp. 329-347.
[13] TdB Consultancy. 2010. *FITC-Dextran Fluorescein isothiocyanate dextran*. [ONLINE] Available at: http://tdbcons.com/images/pdf/fitcdextran2.pdf. [Accessed 29 June 2018].
[14] LV, X., ZHANG, L., XING, F. and LIN, H., 2016. Controlled synthesis of monodispersed mesoporous silica nanoparticles: Particle size tuning and formation mechanism investigation. *Microporous and Mesoporous Materials,* **225**, pp. 238-244.
[15] FOUILLOUX, S., DAILLANT, J. and THILL, A., 2012. Single step synthesis of 5–30 nm monodisperse silica nanoparticles: Important experimental parameters and modeling. *Colloids and Surfaces A: Physicochemical and Engineering Aspects,* **393**, pp. 122-127.
[16] BECK, J., VARTULI, J., KENNEDY, G., KRESGE, C., ROTH, W. and SCHRAMM, S., 1995. Molecular Or Supramolecular Templating: Defining The Role of Surfactant Chemistry In the Formation of M41S and Zeolitic Molecular Sieves. *Studies in Surface Science and Catalysis.* Elsevier, pp. 15-16.
[17] PRABHAKAR, N., 2018. Facilated cancer imaging applications, Pharmaceutical Nanotechnology Course, Åbo Akademi, Auditorium Biokemi.
[18] PRABHAKAR, N., 2018. Multimodal imaging probes and delivery systems for cancer nanomedicine.
[19] TARN, D., ASHLEY, C.E., XUE, M., CARNES, E.C., ZINK, J.I. and BRINKER, C.J., 2013. Mesoporous silica nanoparticle nanocarriers: biofunctionality and biocompatibility. *Accounts of Chemical Research,* **46**(3), pp. 792-801.
[20] LI, Z., NYALOSASO, J.L., HWANG, A.A., FERRIS, D.P., YANG, S., DERRIEN, G., CHARNAY, C., DURAND, J. and ZINK, J.I., 2011. Measurement of uptake and release capacities of mesoporous silica nanoparticles enabled by nanovalve gates. *The Journal of Physical Chemistry C,* **115**(40), pp. 19496-19506.
[21] Drugbank. 2005. *Fluorescein*. [ONLINE] Available at: https://www.drugbank.ca/drugs/DB00693. [Accessed 29 June 2018].
[22] HERMANSON, G.T., 2013. *Bioconjugate techniques.* Academic press.
[23] HILGERT, E., 2015. *Development of Pharmaceutical Ink Formulations with Silica Nanoparticles for Inkjet Printing.*
[24] ZANJANCHI, M.A. and JABARIYAN, S., 2014. Application of ultrasound and methanol for the rapid removal of surfactant from MCM-41 molecular sieve. *Journal of the Serbian Chemical Society,* **79**(1), pp. 25.

[25] LANG, N. and TUEL, A., 2004. A fast and efficient ion-exchange procedure to remove surfactant molecules from MCM-41 materials. *Chemistry of materials,* **16**(10), pp. 1961-1966. [26] ROSENHOLM, J., 2018. Characterization of Nanomaterials, Pharmaceutical Nanotechnology Course, Åbo Akademi, Auditorium Biokemi.

[27] NanoComposix. Eu. 2018. *Characterization Techniques*. [ONLINE] Available at: https://nanocomposix.eu/pages/characterization-techniques. [Accessed 29 June 2018].

[28] KAASALAINEN, M., ASEYEV, V., VON HAARTMAN, E., KARAMAN, D.Ş., MÄKILÄ, E., TENHU, H., ROSENHOLM, J. and SALONEN, J., 2017. Size, stability, and porosity of mesoporous nanoparticles characterized with light scattering. *Nanoscale research letters,* **12**(1), pp. 74.

[29] KIM, J., KIM, L. and KIM, C., 2007. Size control of silica nanoparticles and their surface treatment for fabrication of dental nanocomposites. *Biomacromolecules,* **8**(1), pp. 215-222.

[30] XU, P., WANG, H., TONG, R., DU, Q. and ZHONG, W., 2006. Preparation and morphology of SiO 2/PMMA nanohybrids by microemulsion polymerization. *Colloid and Polymer Science,* **284**(7), pp. 755-762.

[31] Imaging & Microscopy, MICHEN, B., BALOG, S., ROTHEN-RUTISHAUSER, B., PETRI-FINK, A., VANHECKE, D., 2014. *TEM Sample Preparation of Nanoparticles in Suspensions Understanding the Formation of Drying Artefacts. [ONLINE] Available at: https://www.imaging-git.com/science/electron-and-ion-microscopy/tem-sample-preparation-nanoparticles-suspensions*. [Accessed 29 June 2018].

[32] MA, M., 2018, Mesoporous silica materials in pharmaceutical nanotechnology , Pharmaceutical Nanotechnology Course, Åbo Akademi, Auditorium Farmaci.

[33] BANSAL, K., 2018, Smart polymers for drug delivery, Pharmaceutical Nanotechnology Course, Åbo Akademi, Auditorium Farmaci.

[34] FROHLICH, E., 2012. The role of surface charge in cellular uptake and cytotoxicity of medical nanoparticles. *International journal of nanomedicine,* **7**, pp. 5577-5591.

[35] ROSENHOLM, J.M., DUCHANOY, A. and LINDÉN, M., 2007. Hyperbranching surface polymerization as a tool for preferential functionalization of the outer surface of mesoporous silica. *Chemistry of Materials,* **20**(3), pp. 1126-1133.

[36] KIM, C.O., CHO, S.J. and PARK, J.W., 2003. Hyperbranching polymerization of aziridine on silica solid substrates leading to a surface of highly dense reactive amine groups. *Journal of colloid and interface science,* **260**(2), pp. 374-378.

[37] XIA, T., KOVOCHICH, M., LIONG, M., MENG, H., KABEHIE, S., GEORGE, S., ZINK, J.I. and NEL, A.E., 2009. Polyethyleneimine coating enhances the cellular uptake of mesoporous silica nanoparticles and allows safe delivery of siRNA and DNA constructs. *ACS nano,* **3**(10), pp. 3273-3286. [38] CILURZO, F., MINGHETTI, P., CASIRAGHI, A., TOSI, L., PAGANI, S. and MONTANARI, L., 2005. Polymethacrylates as crystallization inhibitors in monolayer transdermal patches containing ibuprofen. *European Journal of Pharmaceutics and Biopharmaceutics,* **60**(1), pp. 61-66.
[39] NEWMAN, A.W. and BYRN, S.R., 2003. Solid-state analysis of the active pharmaceutical ingredient in drug products. *Drug discovery today,* **8**(19), pp. 898-905.
[40] AMBROGI, V., PERIOLI, L., MARMOTTINI, F., ACCORSI, O., PAGANO, C., RICCI, M. and ROSSI, C., 2008. Role of mesoporous silicates on carbamazepine dissolution rate enhancement. *Microporous and Mesoporous Materials,* **113**(1-3), pp. 445-452.
[41] LIMNELL, T., SANTOS, H.A., MÄKILÄ, E., HEIKKILÄ, T., SALONEN, J., MURZIN, D.Y., KUMAR, N., LAAKSONEN, T., PELTONEN, L. and HIRVONEN, J., 2011. Drug delivery formulations of ordered and nonordered mesoporous silica: comparison of three drug loading methods. *Journal of pharmaceutical sciences,* **100**(8), pp. 3294-3306.
[42] JANG, D., KIM, D. and MOON, J., 2009. Influence of fluid physical properties on ink-jet printability. *Langmuir,* **25**(5), pp. 2629-2635.
[43] KUSCER, D., STAVBER, G., TREFALT, G. and KOSEC, M., 2012. Formulation of an aqueous titania suspension and its patterning with ink-jet printing technology. *Journal of the American Ceramic Society,* **95**(2), pp. 487-493.
[44] RAIJADA, D., GENINA, N., FORS, D., WISAEUS, E., PELTONEN, J., RANTANEN, J. and SANDLER, N., 2013. A step toward development of printable dosage forms for poorly soluble drugs. *Journal of pharmaceutical sciences,* **102**(10), pp. 3694-3704.
[45] WICKSTRÖM, H., HILGERT, E., NYMAN, J.O., DESAI, D., ŞEN KARAMAN, D., DE BEER, T., SANDLER, N. and ROSENHOLM, J.M., 2017. Inkjet Printing of Drug-Loaded Mesoporous Silica Nanoparticles—A Platform for Drug Development. *Molecules,* **22**(11), pp. 2020.
[46] Selleckchem.com. (2018). *Nirogacestat (PF-03084014, PF-3084014)* | *Gamma-secretase inhibitor* | *Read Reviews & Product Use Citations.* [online] Available at: http://www.selleckchem.com/products/pf-03084014-pf-3084014-html [Accessed 10 Aug. 2018].

[47] HYVÄLUOMA, J., KEMPPINEN, T., HAAVISTO, S., RAISKINMA, P., TOIVAKKA, M., KATAJA, M., 2003, Rheology of liquid particle suspensions (ReoMaT – project).
[48] PARK, J. and MOON, J., 2006. Control of colloidal particle deposit patterns within picoliter droplets ejected by ink-jet printing. *Langmuir,* **22**(8), pp. 3506-3513. [49] SING, K., 2001. The use of nitrogen adsorption for the characterization of porous materials. *Colloids and Surfaces A: Physicochemical and Engineering Aspects,* **187**, pp. 3-9.
[50] ESER, A., DUARTE CAMPOS, D.F., PUSTER, U., RICHTERING, W., STEVENS, M.M. and FISCHER, H., 2016. Controlling shear stress in 3D bioprinting is a key factor to balance printing resolution and stem cell integrity. *Advanced healthcare materials,* **5**(3), pp. 326-333.
[51] Denovix.com. (2018). *Baseline Correction Technical Note.* [online] Available at: https://www.denovix.com/pdf/119-Baseline-Correction.pdf [Accessed 9 Aug. 2018].
[52] POLYETHYLENEIMINE, BRANCHED | 9002-98-6 [Internet]. Chemicalbook.com. 2018 [cited 10 August 2018]. Available from: http://www.chemicalbook.com/ChemicalProductsProperty_EN_CB9162514.htm
[53] Cetyltrimethylammonium bromide | C19H42BrN | ChemSpider [Internet]. Chemspider.com. 2018 [cited 10 August 2018]. Available from: http://www.chemspider.com/Chemical-Structure.5754.html
[54] DESAI, D., KARAMAN, D.S., PRABHAKAR, N., TADAYON, S., DUCHANOY, A., TOIVOLA, D.M., RAJPUT, S., NÄREOJA, T. and ROSENHOLM, J.M., 2014. Design considerations for mesoporous silica nanoparticulate systems in facilitating biomedical applications. *Open Material Sciences,* **1**(1),.
[55] TAKAKUSA, H., KIKUCHI, K., URANO, Y., HIGUCHI, T. and NAGANO, T., 2001. Intramolecular fluorescence resonance energy transfer system with coumarin donor included in β-cyclodextrin. *Analytical Chemistry,* **73**(5), pp. 939-942.
[56] CORNIER, J., OWEN, A., KWADO, A., VAN DE VOORDE, M., 2017. Pharmacetuical Nanotechnology, Innovation and Production, *WILEY VCH.*
[57] SALEH, N., YOUSAF, Z., 2018. Tools and techniques for the optimized synthesis, reproducibility and scale up of desired nanoparticles from plant derived material and their role in pharmaceutical properties. WILEY VCH, pp.85-131.
[58] Carlroth.com. (2018). γ-Aminopropyltriethoxysilane (APTES) | γ-Aminopropyltriethoxysilane (APTES) | A | A-Z Chemicals | Chemicals | PZ_XML_Export_EN_Web | XML_EN_44 | International. [online] Available at:

https://www.carlroth.com/en/en/Chemicals/A-Z-Chemicals/A/%CE%B3-Aminopropyltriethoxysilane-%28APTES%29/%CE%B3-Aminopropyltriethoxysilane-%28APTES%29/p/000000000001ade600030023_en [Accessed 27 Sep. 2018].

[59] PREIS, M., ROSENHOLM, J.M., 2017. *Printable nanomedicines: the future of customized drug delivery?*

[60] BRINKER, C. J., SCHERER, G. W., Sol-gel science: the physics and chemistry of sol-gel processing, 1990. 1st edition. Elsevier.

[61] YAN, W., ZHANG, Z., GOU, X., LIU, W., SONGA, Z., The Effect of pH on Sapphire Chemical Mechanical Polishing, 2015. *ECS Journal of Solid State Science and Technology,* 4(3) P108-P111.

[62] AG, L. (2018). *Dynamic Light Scattering*. [online] Lsinstruments.ch. Available at: https://lsinstruments.ch/en/technology/dynamic-light-scattering-dls [Accessed 8 Oct. 2018].

[63] VAZQUE, N. I., GONZALEZ, Z., FERRARI, B., CASTRO, Y., 2017. Synthesis of mesoporous silica nanoparticles by sol-gel as nanocontainer for future drug delivery applications, *Boletìn de la Sociedad Espanola de Ceramica y Vidro,* pp.139-145.

8. APPENDIX

Appendix 1: detailed synthesis protocol of MSNs (in the brackets the adding order)

1. Non-labeled MSNs

Reaction solution: 160 mL H_2O (1) + 0.41 g CTAB (2) + 0.116 g NaOH (3) + 40 mL Etax Aa (4) + 2.1mL TEOS (5) at 33°C during overnight stirring

2. 1% APTES-FITC MSNs

Reaction Solution:

160 mL H_2O (1) + 0.41 g CTAB (2) + 0.116 g NaOH (3) + 38 mL Etax Aa (4) + 2.1 mL TEOS (5)

Conjugation Solution:

2 mL Etax Aa (1) + 24 mg FITC (2) + 22 μL APTES (3)

3. 5% APTES-FITC MSNs

Reaction Solution:

160 mL H_2O (1) + 0.41 g CTAB (2) + 0.116 g NaOH (3) + 38 mL Etax Aa (4) + 2.1 mL TEOS (5)

Conjugation Solution:

2 mL Etax Aa (1) + 24 mg FITC (2) + 110μL APTES (3)

4. 10% APTES-FITC MSNs

Reaction Solution:

160 mL H_2O (1) + 0.41 g CTAB (2) + 0.116 g NaOH (3) + 38 mL Etax Aa (4) + 2.1 mL TEOS (5)

Conjugation Solution:

2 mL Etax Aa (1) + 24 mg FITC (2) + 220 μL APTES (3)

5. 1% APTES-FITC MSNs (400 mL)

Reaction Solution:

320 mL H_2O (1) + 0.832 g CTAB (2) + 0.232 g NaOH (3) + 78 mL EtOH (4) + 4.4 mL TEOS (5)

Conjugation Solution:

2mL EtOH (1) + 24.4 mg FITC (2) + 44 μL APTES (3)

Appendix 2: Trasmission Electron Microscope images of the batches.

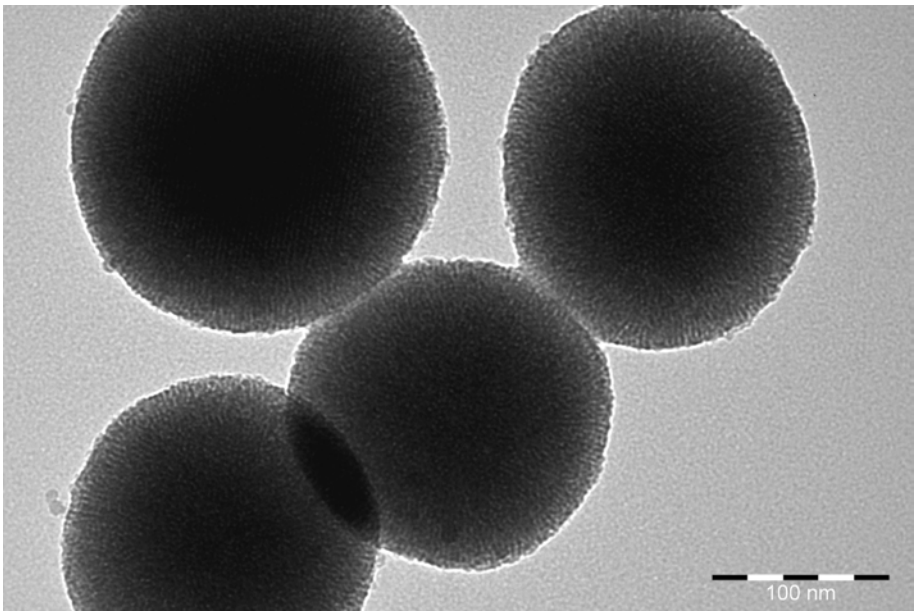

Fig. 8.1. Bare MSNs.

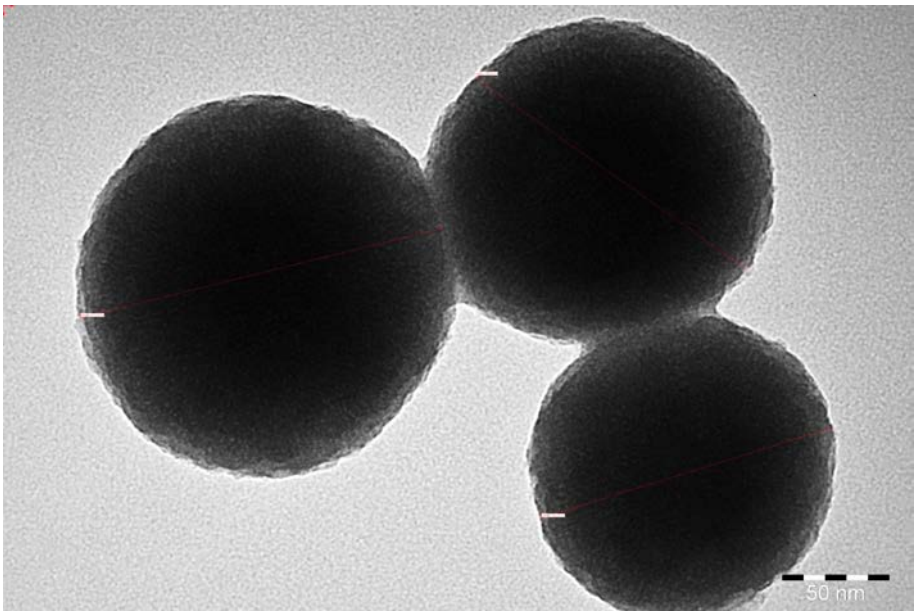

Fig. 8.2. 5 % APTES-FITC MSNs.

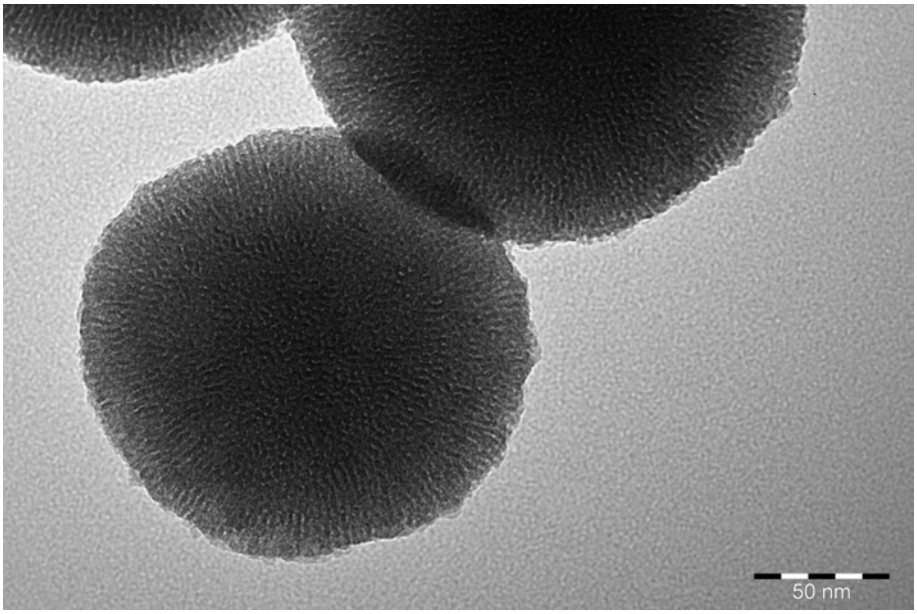

Fig. 8.3. 10% APTES-FITC MSN

Acknowledgement

It couldn’t have been a better conclusion of these university years than staying in a such peaceful country, as Finland. I’d like to thank all the people who have made me so welcomed there. In particular, I will always be grateful to Professor Jessica Rosenholm, who gave me the opportunity to carry out the thesis on a different, compared to my previous studies, as well as very interesting topic as nanomedicine. I would also like to express my infinite gratitude to Prakirth Govardhanam and Henrika Wickström. They have guided me through this project, by letting me enjoy my experience. I would also thank professor Paolo Canu who has always been available showing a great professionalism. During these five years there have been many ups and downs, but nothing could be so successful without the support of my family, my father, my mother and my sister and my dear friends, Samantha, Cristian and Riccardo, that especially in this period abroad have been fundamental for me. It was a pleasure to make you proud of me. Last but not least I would also like to thank Claudio and all my huge number of friends I spent time with, here and abroad.